Downscaling atmospheric CO_2 measurements into surface fluxes

Philippe Ciais and Philippe Bousquet

How can we estimate CO_2 fluxes ?

Inverse modeling of Atmospheric Transport

Ill-posed problem
Error amplification

DOWNSCALING

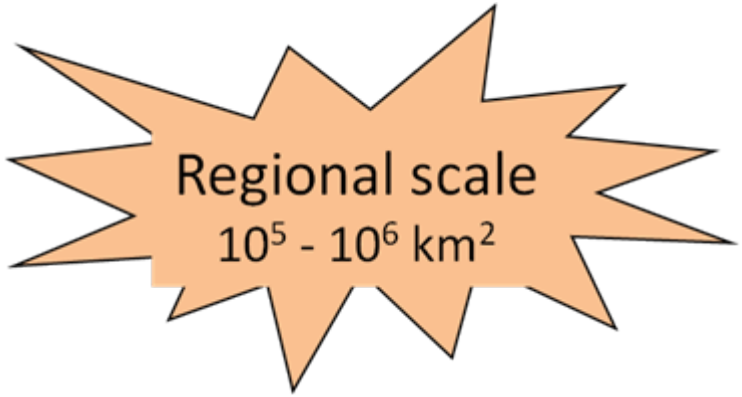

UPSCALING

Extrapolation
Strong heterogeneity

<u>Forest inventories</u>
- local (1ha)

<u>Flux towers</u>
(1-10 km^2)

<u>Ocean studies</u>
Extrapolated ΔpCO_2 measurements

<u>Direct models</u>
- biospheric
- Oceanic
(1-5000 km^2)

Outline

1 - Atmospheric measurements

2 - Data Integration in models

3 - Towards regional flux estimates

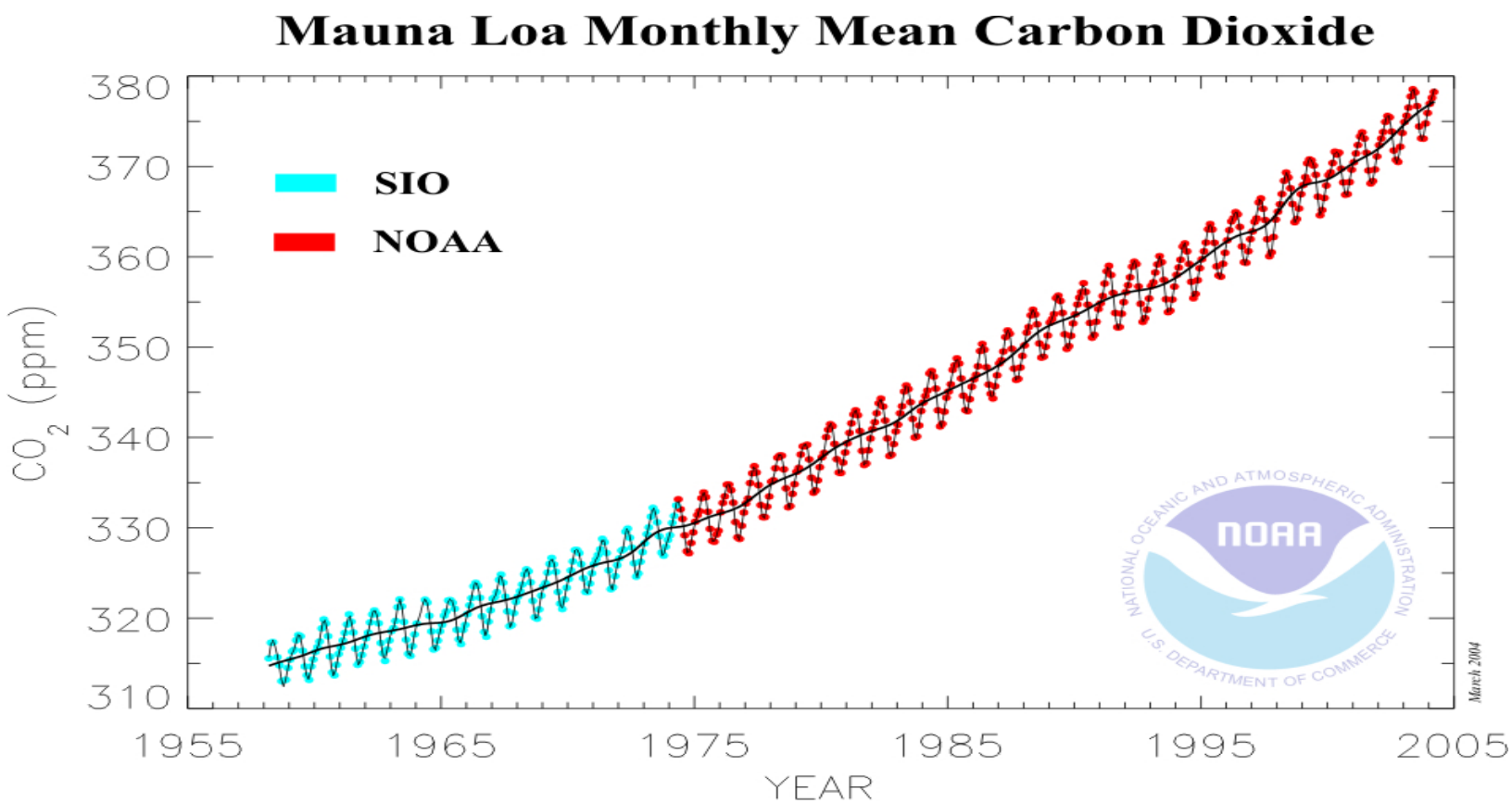

Atmospheric carbon dioxide monthly mean mixing ratios. Data prior to May 1974 are from the Scripps Institution of Oceanography (SIO, blue), data since May 1974 are from the National Oceanic and Atmospheric Administration (NOAA, red). A long-term trend curve is fitted to the monthly mean values. Principal investigators: Dr. Pieter Tans, NOAA CMDL Carbon Cycle Greenhouse Gases, Boulder, Colorado, (303) 497-6678, pieter.tans@noaa.gov, and Dr. Charles D. Keeling, SIO, La Jolla, California, (616) 534-6001, cdkeeling@ucsd.edu.

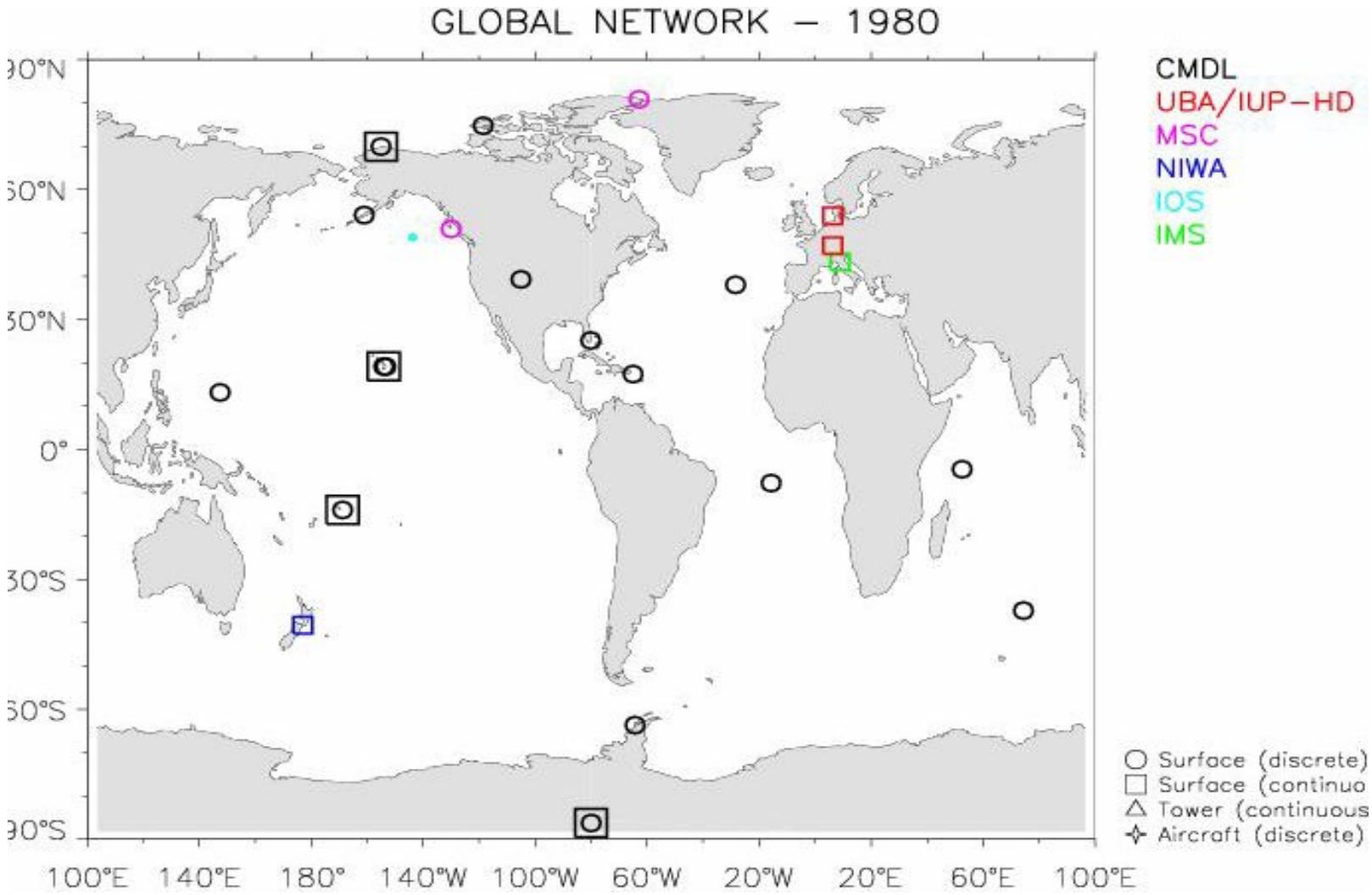

Masarie et Tans

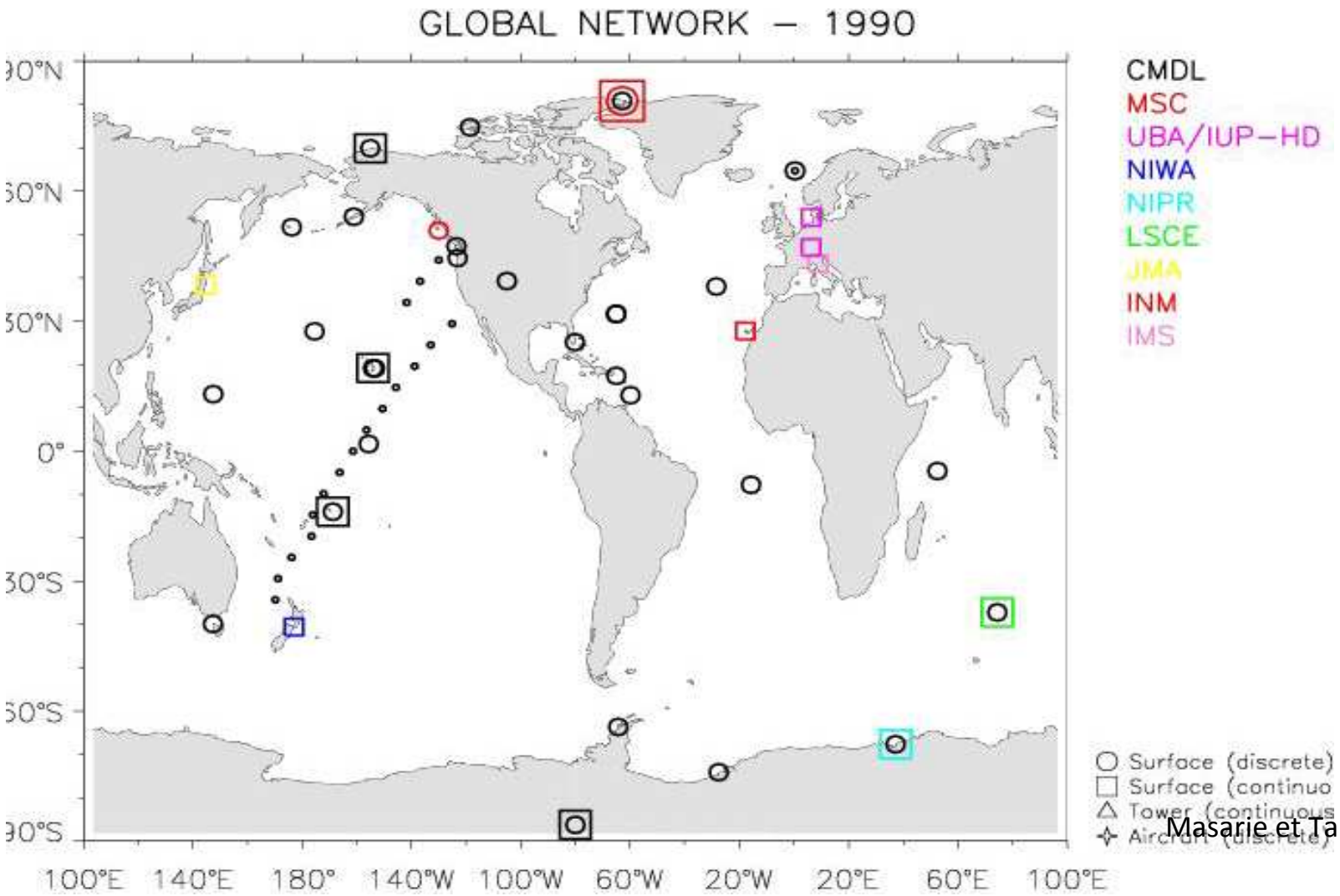

Masarie et Tans

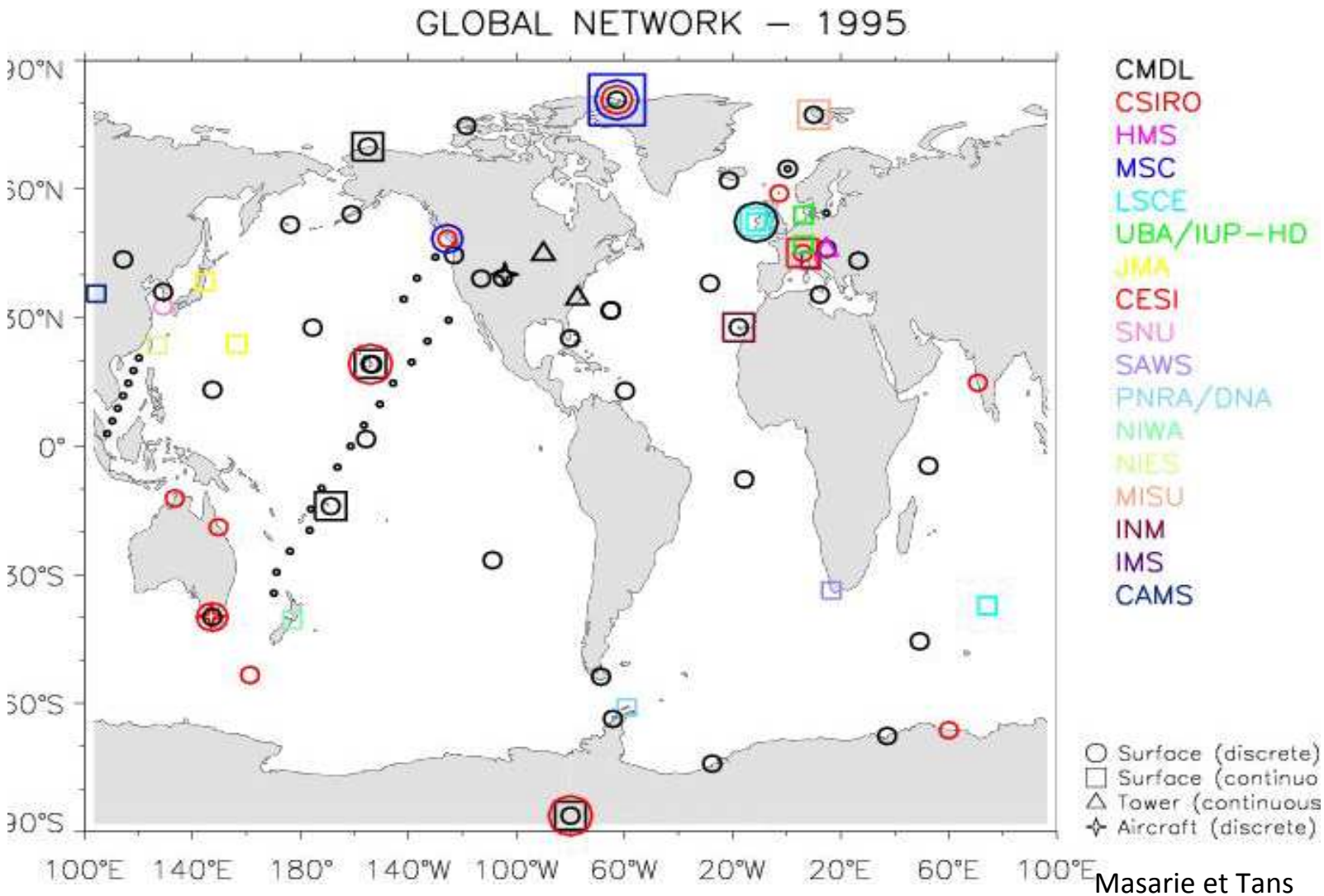

Masarie et Tans

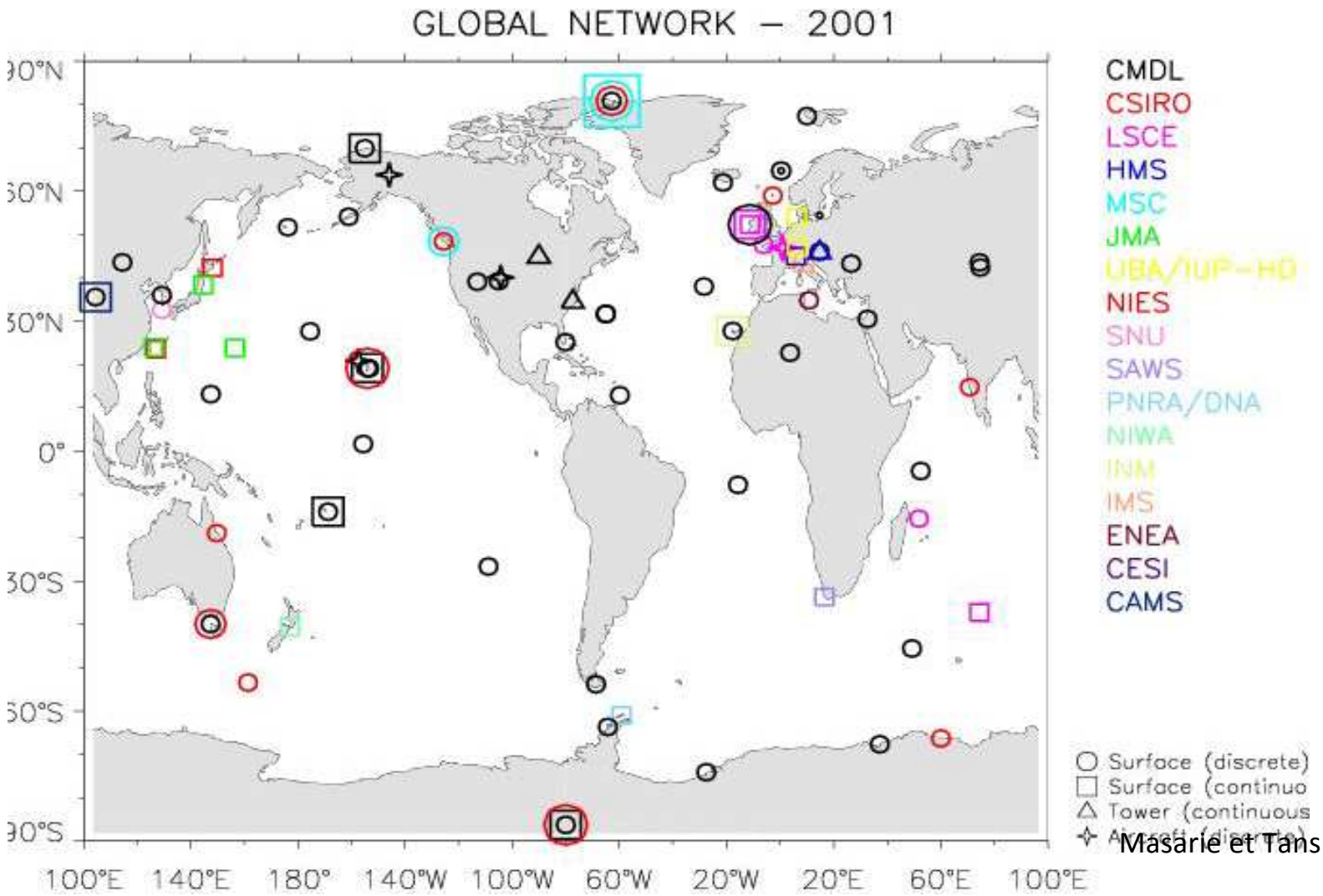

Masarie et Tans

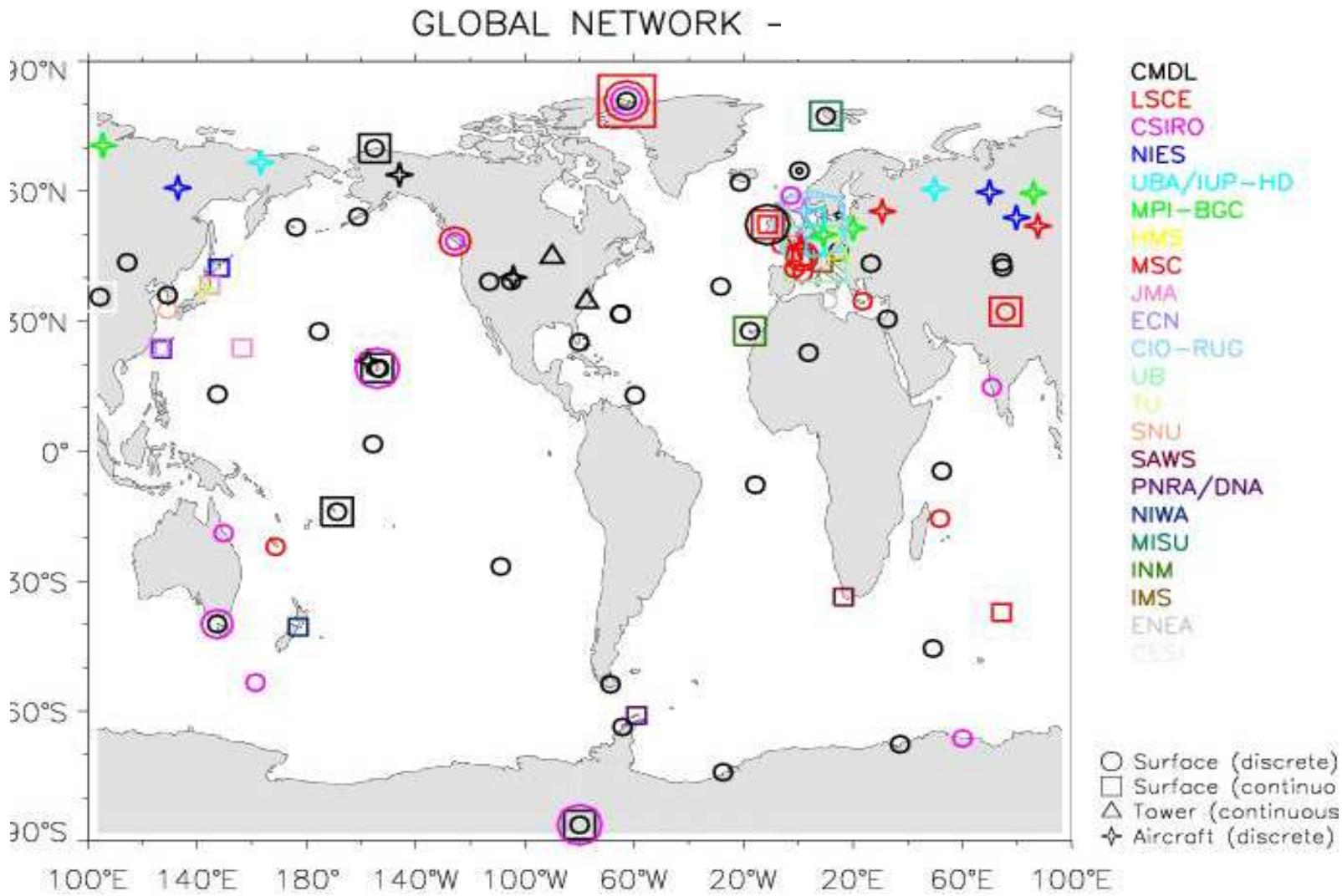
GLOBAL NETWORK -
CMDL
LSCE
CSIRO
NIES
UBA/IUP-HD
MPI-BGC
MSC
JMA
ECN
CIO-RUG
UB
SNU
SAWS
PNRA/DNA
NIWA
MISU
INM
IMS
ENEA
Surface (discrete)
Surface (continuo
Tower (continuous
Aircraft (discrete)
0°
100°E
140°E
180°
140°W
100°W
60°W
20°W
20°E
60°E
100°E

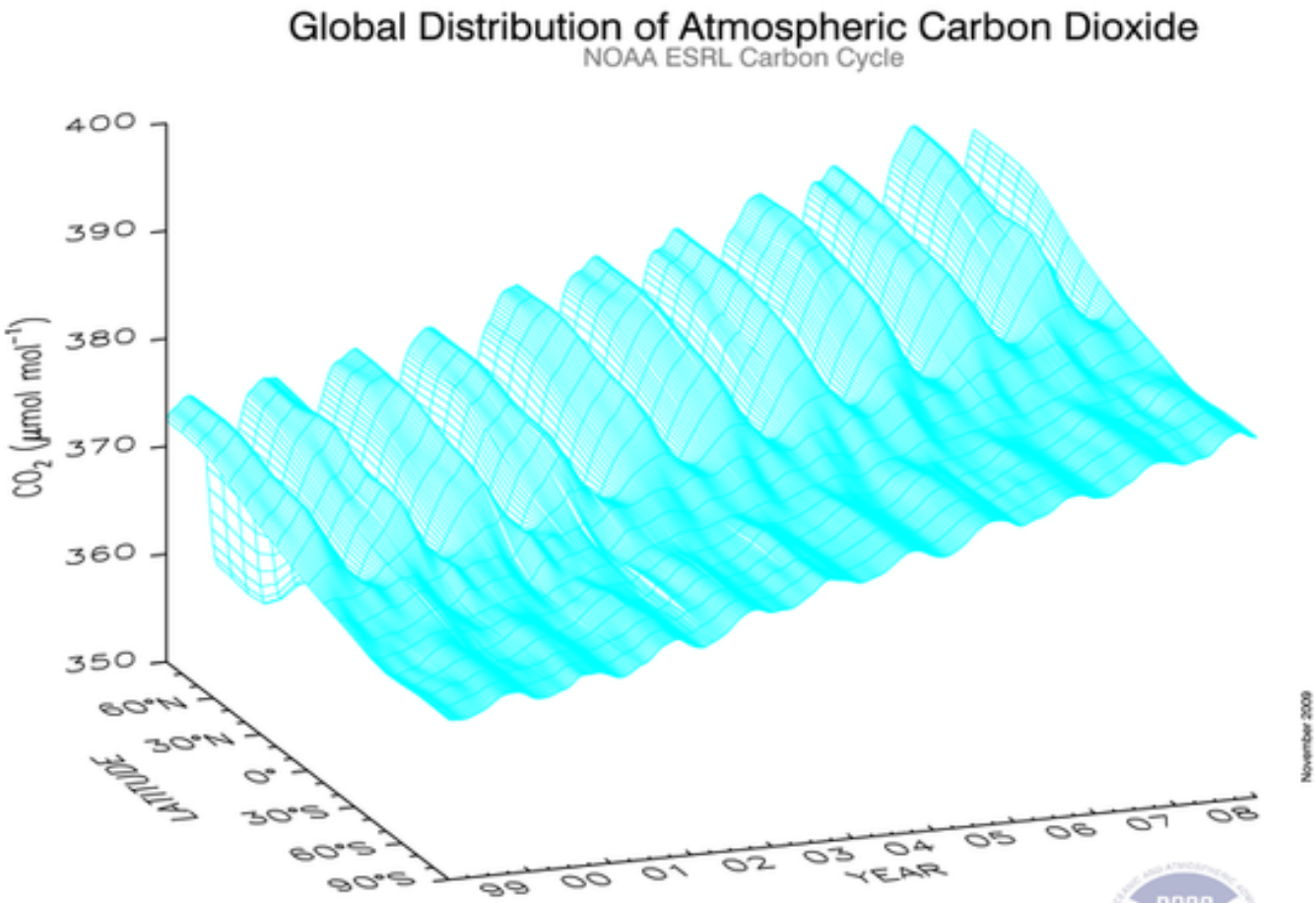
Global Distribution of Atmospheric Carbon Dioxide
NOAA ESRL Carbon Cycle
400
390
380
370
360
350
CO_2 (μmol mol^{-1})
60°N
30°N
0°
30°S
60°S
90°S
LATITUDE
99
00
01
02
03
04
05
06
07
08
YEAR
November 2009
Three-dimensional representation of the latitudinal distribution of atmospheric carbon dioxide in the marine boundary layer. Data from the Carbon Cycle cooperative air sampling network were used. The surface represents data smoothed in time and latitude. Contact: Dr. Pieter Tans and Thomas Conway, NOAA ESRL Carbon Cycle, Boulder, Colorado, (303) 497-6678, pieter.tans@noaa.gov, http://www.esrl.noaa.gov/gmd/ccgg/.
NOAA

Interannual variability

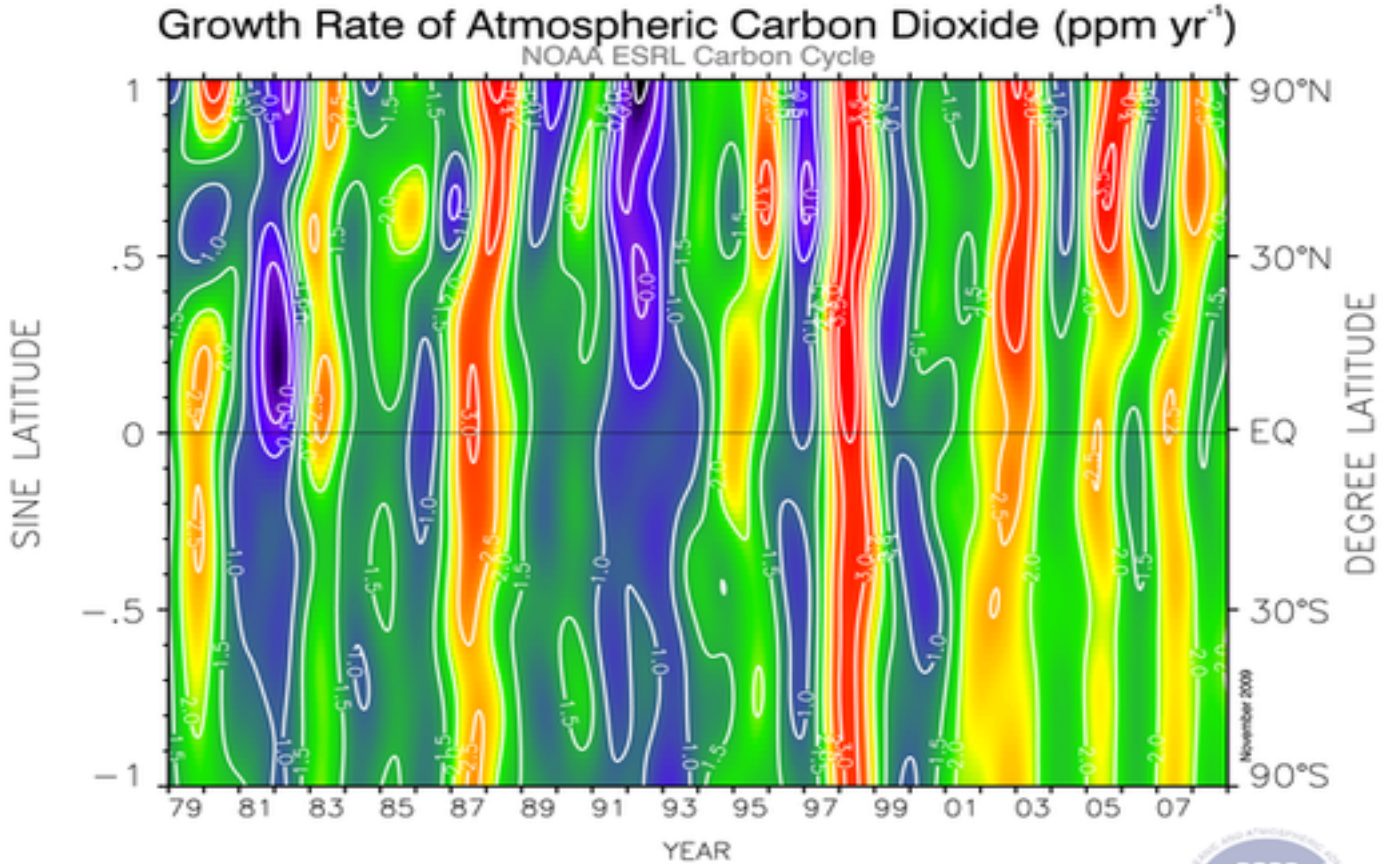

Contour plot showing the temporal and spatial variations in the atmospheric increases of carbon dioxide. The cooler colors (green, blue, violet) represent periods of lower than average growth rates and the warmer colors (yellow, orange, red) represent periods of higher growth rates. The plot is derived from measurements of samples collected at the Carbon Cycle cooperative air sampling network sites. The variations in the growth rate of this climatically important gas are due to interannual variations in the imbalance between sources and sinks, and also to variations in atmospheric transport. Contact: Thomas Conway, NOAA ESRL Carbon Cycle, Boulder, Colorado, (303) 497-6681, thomas.j.conway@noaa.gov, http://www.esrl.noaa.gov/gmd/ccgg/.

Regional dense networks : a challenge for modellers

- Flask ground level sites
- Aircraft profiles
- Aircraft intensive campaigns

- Continuous ground level sites
- High towers
- Multi tracer measurements

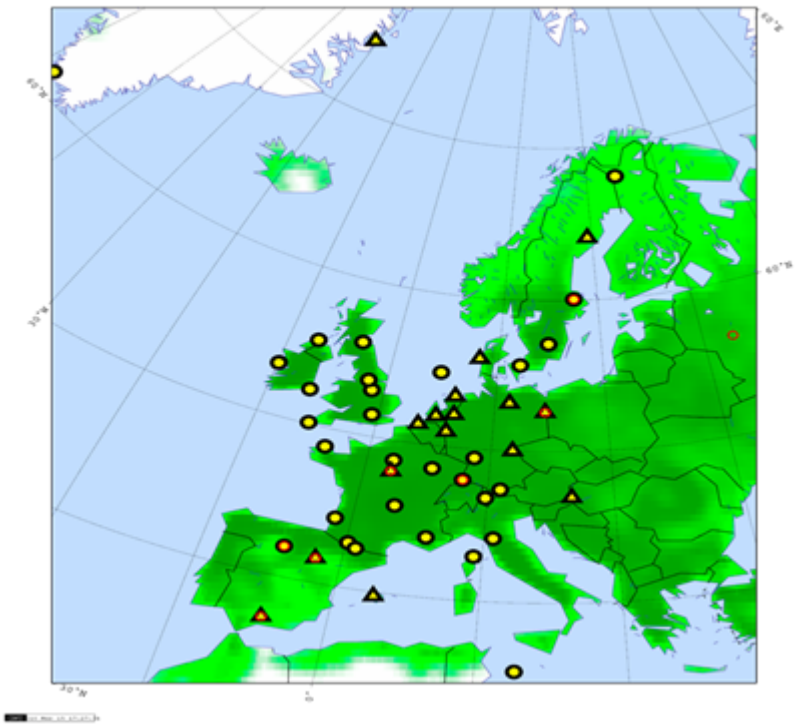

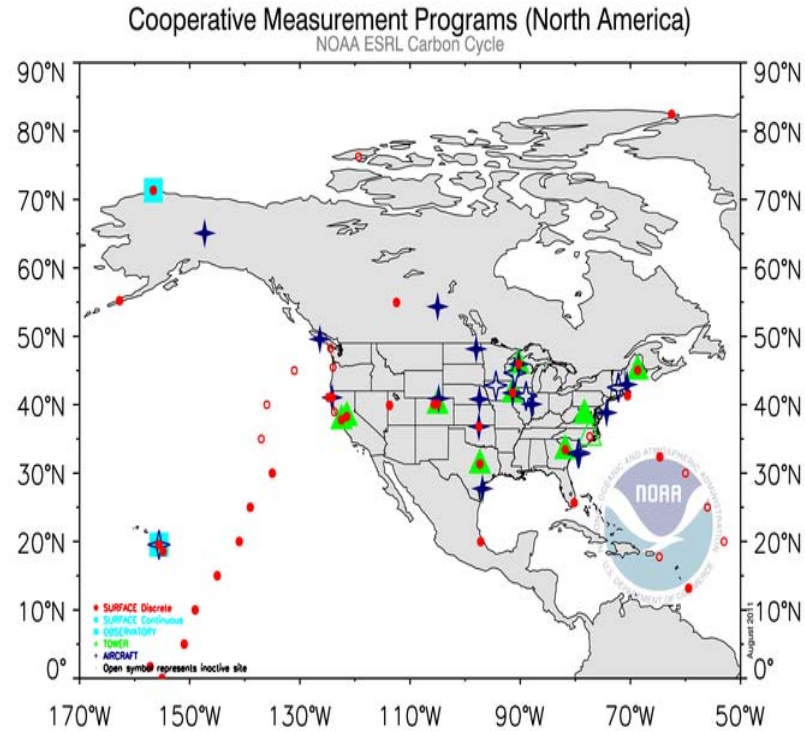

NOAA ESRL Carbon Cycle operates 4 measurement programs. Semi-continuous measurements are made at 4 baseline observatories, a few surface sites and from tall towers. Discrete surface and aircraft samples are measured in Boulder, CO. Presently, atmospheric carbon dioxide, methane, carbon monoxide, hydrogen, nitrous oxide, sulfur hexafluoride, the stable isotopes of carbon dioxide and methane, and halocarbon and volatile organic compounds are measured. Contact: Dr. Pieter Tans, NOAA ESRL Carbon Cycle, Boulder, Colorado, (303) 497-6678, pieter.tans@noaa.gov, http://www.esrl.noaa.gov/gmd/ccgg/.

Aircraft measurements - Orleans, France

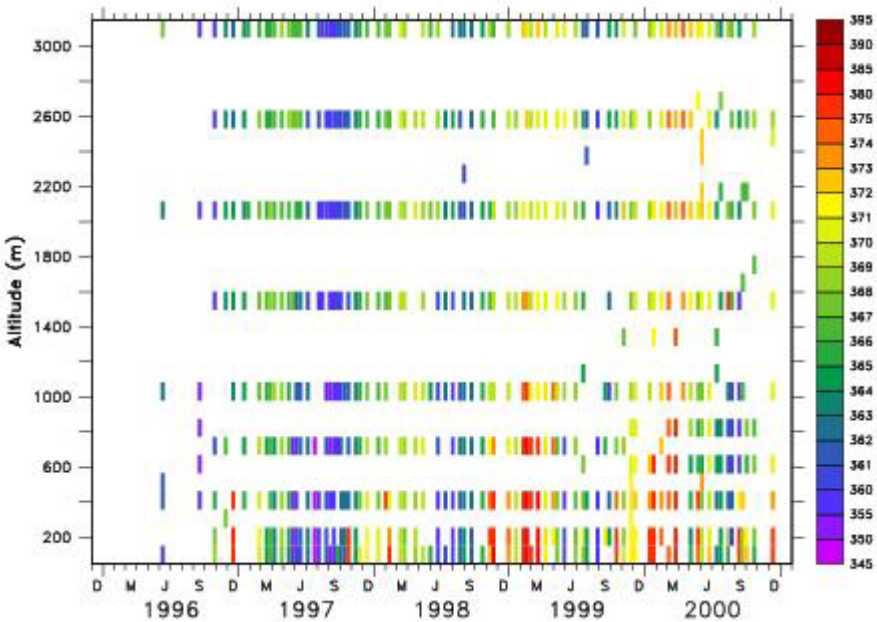

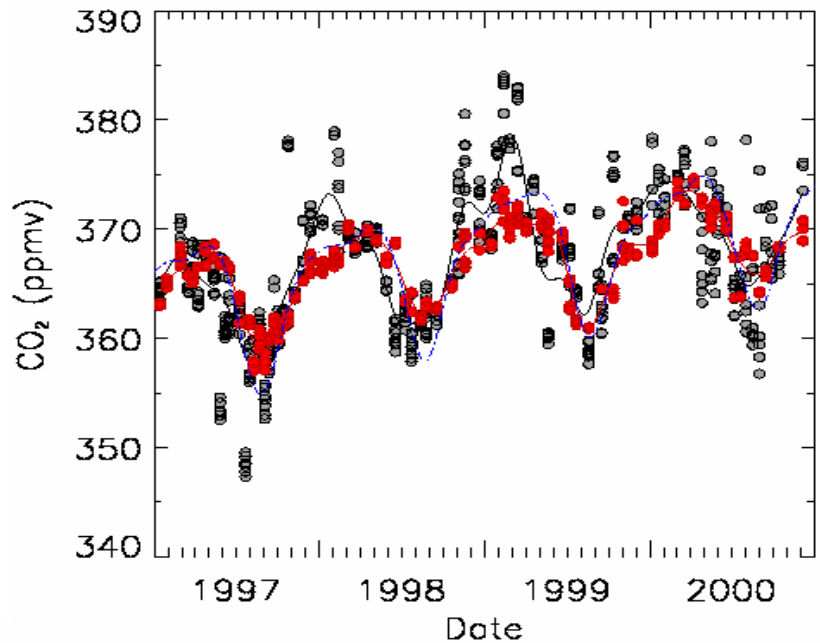

CO2 concentrations
for all monthly flights

CO2 concentrations :

- Boundary layer
- Free troposphere

Aircraft measurements, over United States

Flight over active vegetation

Flight over water stressed vegetation

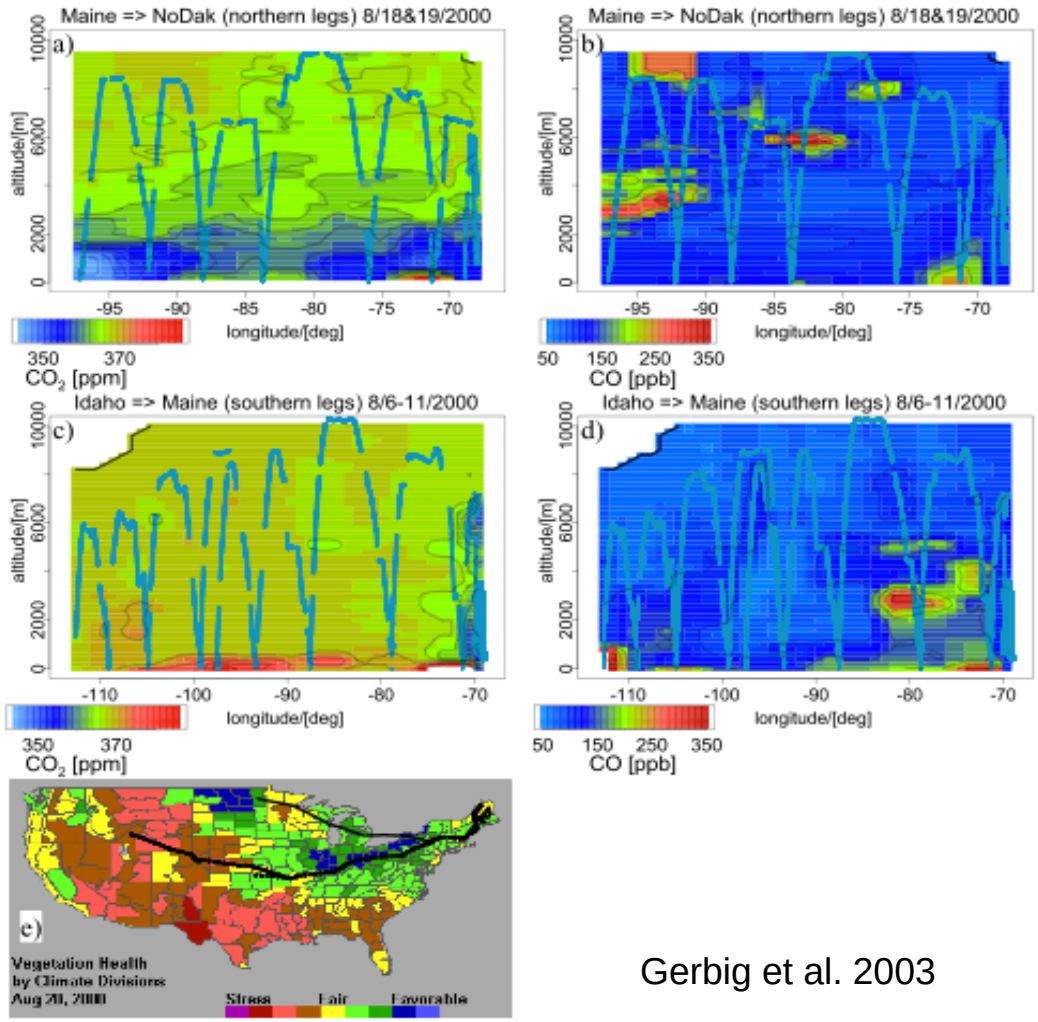

Gerbig et al. 2003

High towers continuous measurements

Footprint area of 7 towers in Europe - CHIOTTO project

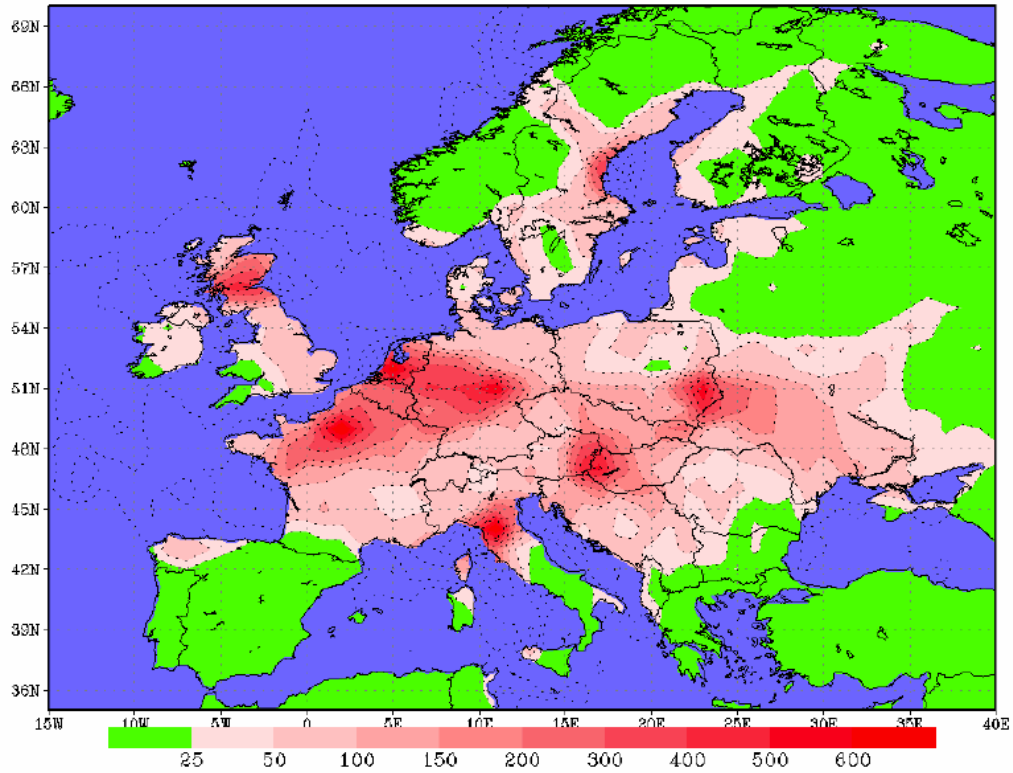

Others tracers, other constraints

O_2/N_2

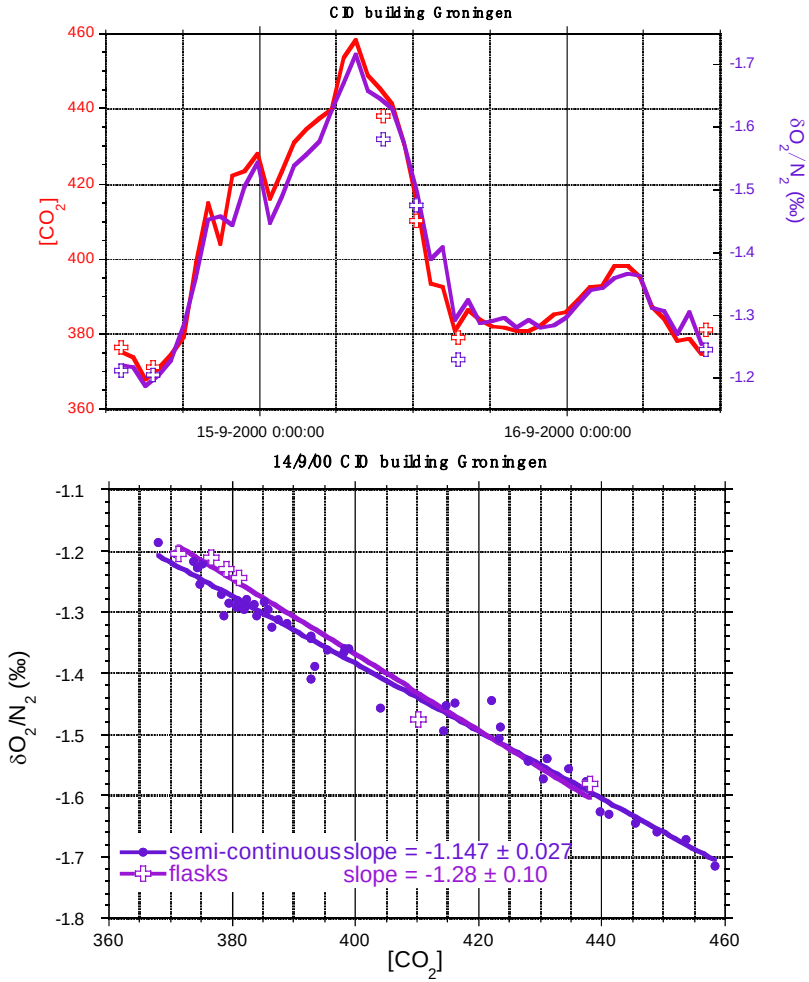

^{14}C in CO_2

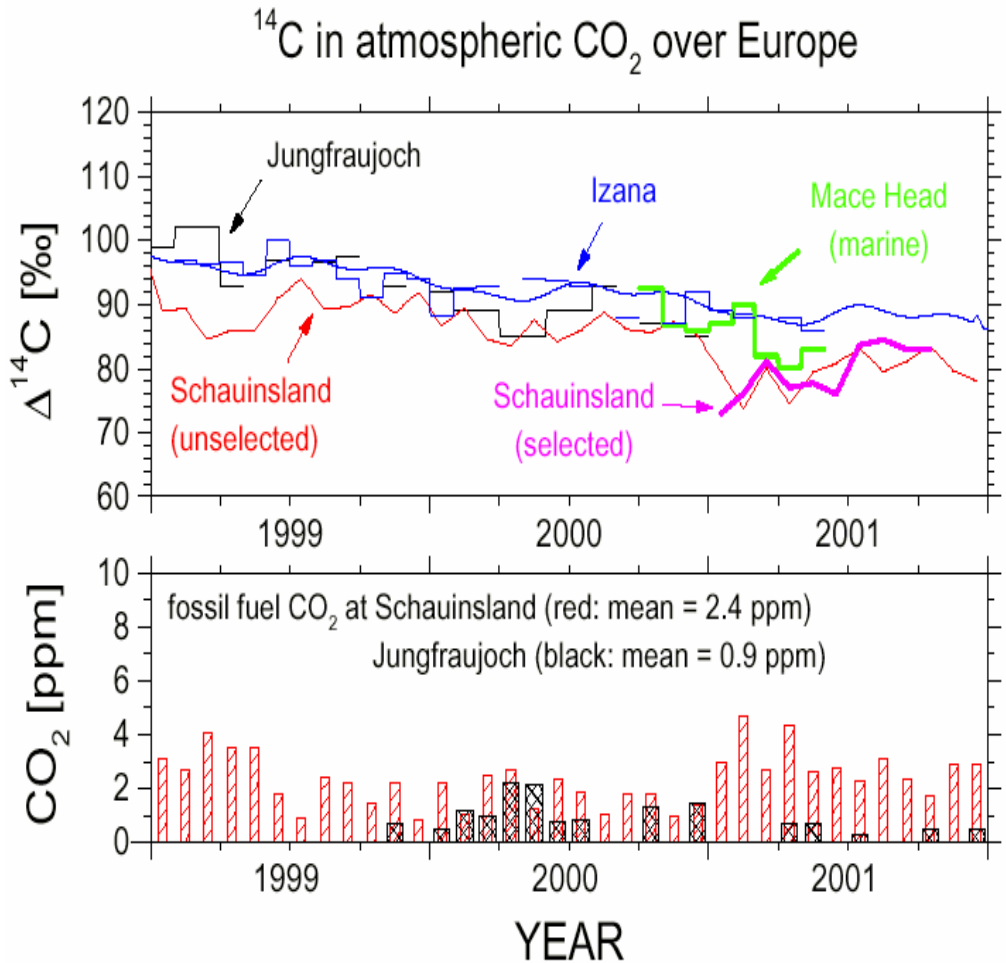

Global network

- Has delivered most of our knowledge on large scale budgets
- Advantage of multiple species measurements
- Uneven coverage, still sparse over some regions
- As more laboratories become involved, calibration and intercomparability becomes crucial
- Continuous measurements under-utilized by models (calibrations, meta-data)

GLOBAVIEW database : http://www.cmdl.noaa.gov/ccgg/globalview/co2/index.html

1 - Atmospheric measurements

2 - Data Integration in models

3 - Towards regional estimates

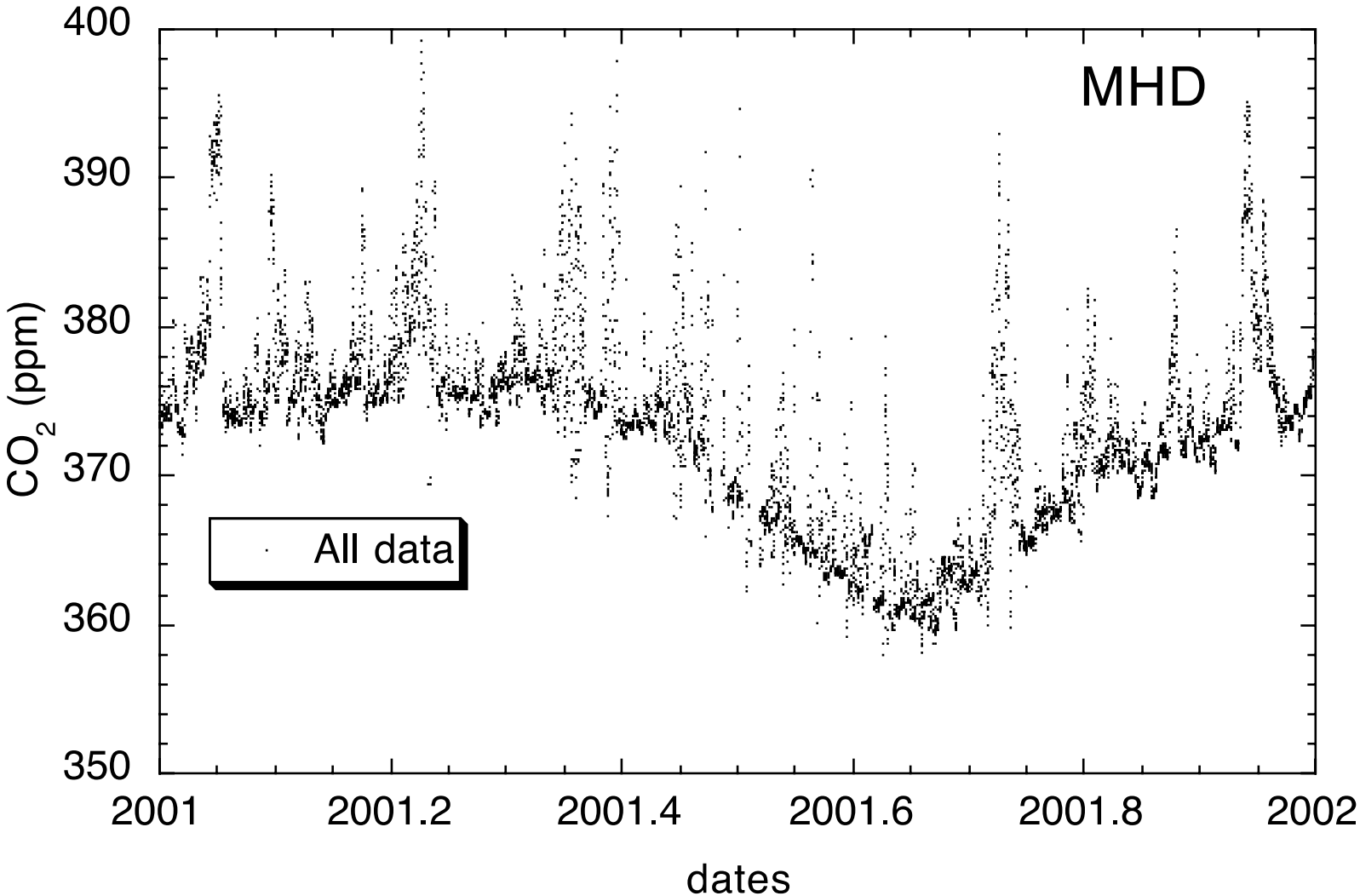
MHD
All data
400
390
380
370
360
350
CO_2 (ppm)
2001
2001.2
2001.4
2001.6
2001.8
2002
dates

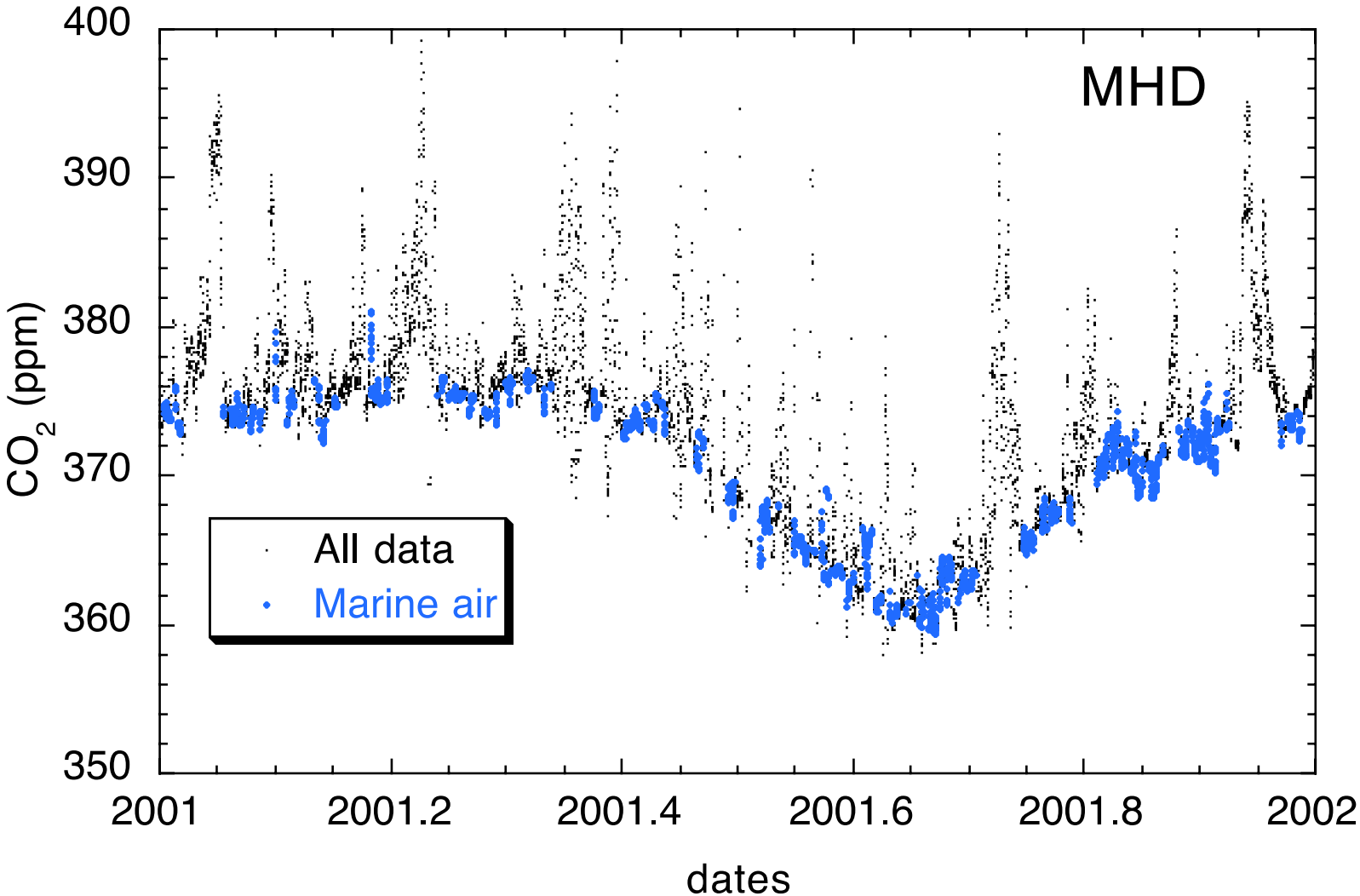
MHD
All data
Marine air
400
390
380
370
360
350
CO_2 (ppm)
2001
2001.2
2001.4
2001.6
2001.8
2002
dates

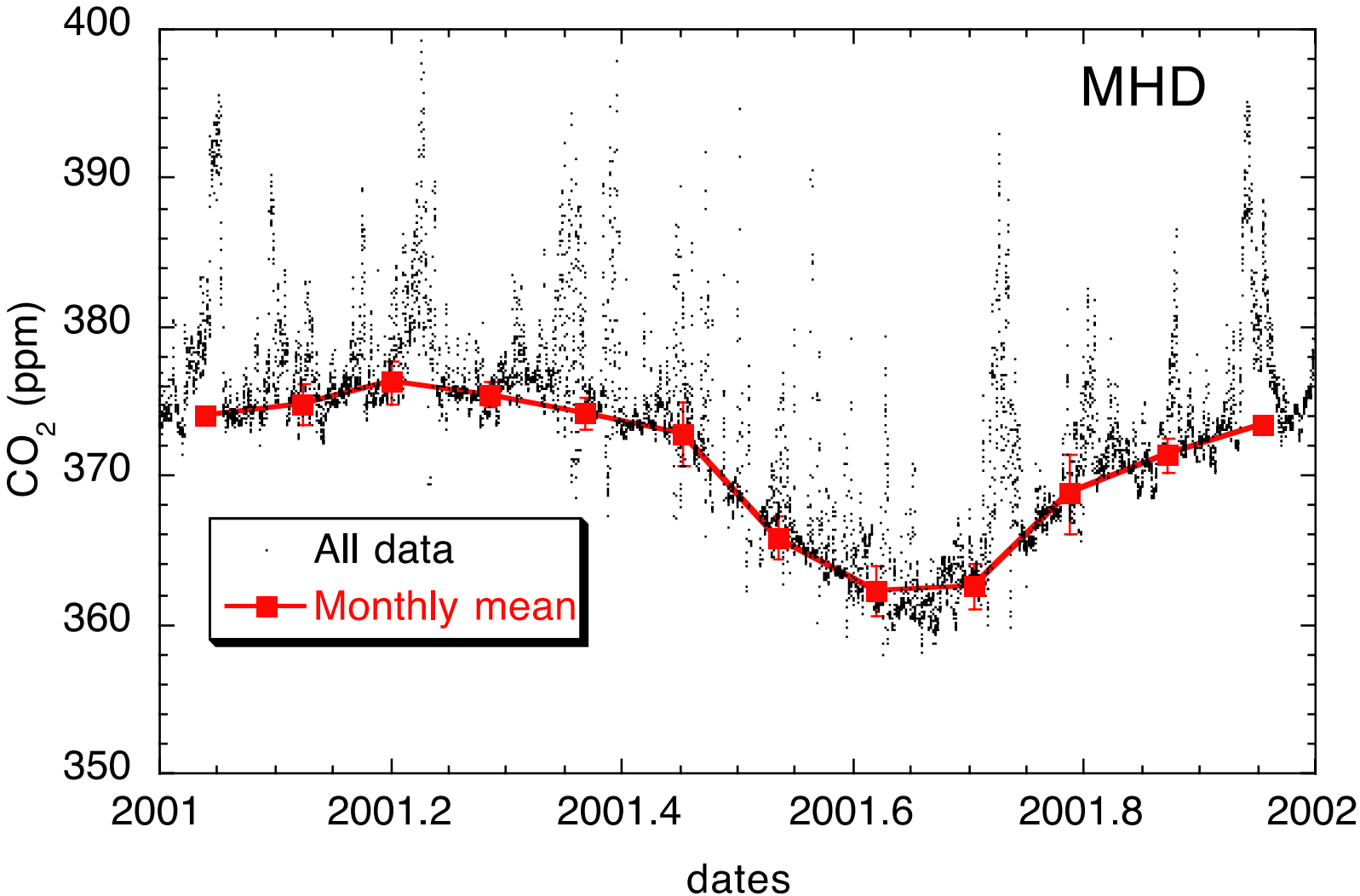
MHD
400
390
380
370
360
350
CO_2 (ppm)
2001
2001.2
2001.4
2001.6
2001.8
2002
dates
All data
Monthly mean

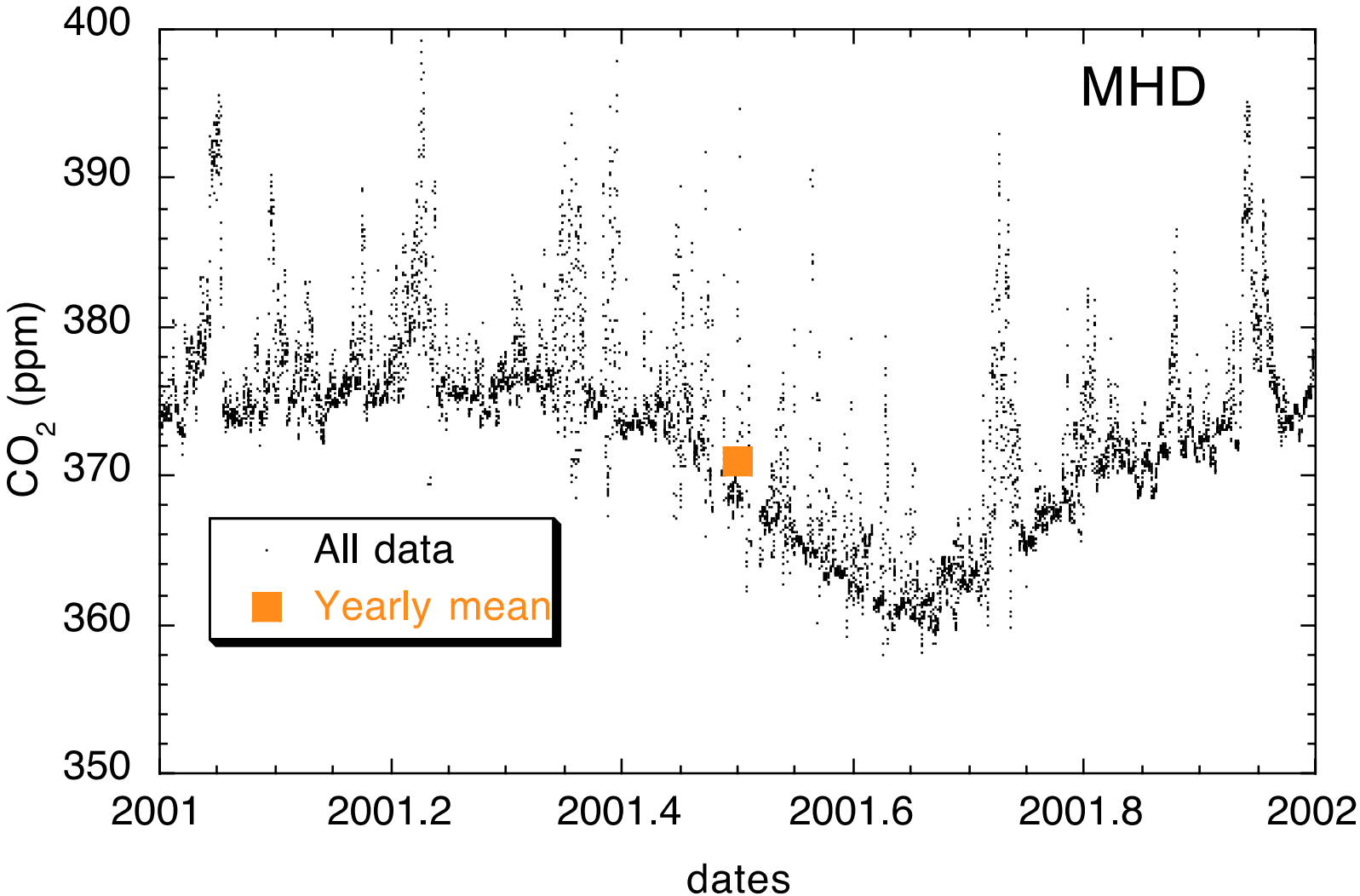
MHD
400
390
380
370
360
350
CO_2 (ppm)
2001
2001.2
2001.4
2001.6
2001.8
2002
dates
All data
Yearly mean

The early 1990's : inversions of annual mean CO_2

Yearly flux estimates
« Large » regions

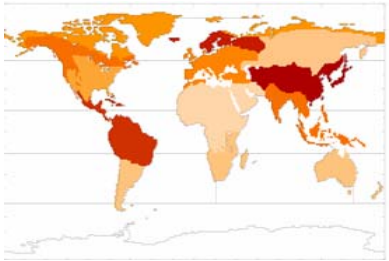

Monthly flux estimates
« Large » regions

Monthly flux estimates
model resolution or small regions

Transport model

Coarse global models

Global high resolution models,
zoomable or regional models

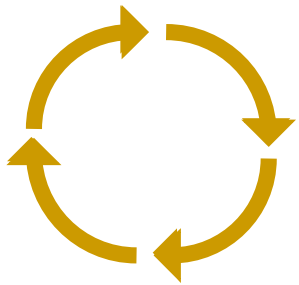

Surface
fluxes

annual
Atmospheric
concentrations

Yearly observations
MBL & coastal sites

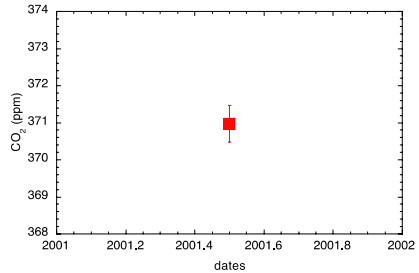

Monthly observations
MBL & coastal sites

Synoptic observations
All sites (continental)

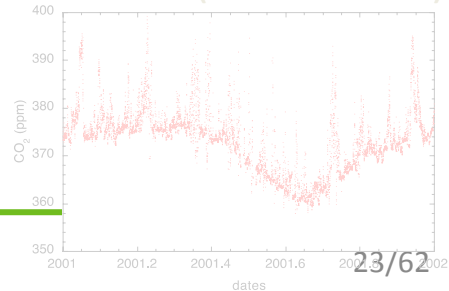

Inverse modeling of discrete sources for a passive tracer

$$\begin{pmatrix} y_1 \\ y_2 \\ . \\ . \\ y_n \end{pmatrix} = \begin{pmatrix} H_{11} & H_{12} & . & . & H_{1m} \\ H_{21} & H_{22} & . & . & H_{2m} \\ . & . & . & . & . \\ . & . & . & . & . \\ H_{n1} & H_{n2} & . & . & H_{nm} \end{pmatrix} \begin{pmatrix} x_1 \\ x_2 \\ . \\ . \\ x_m \end{pmatrix}$$

- 3D numerical model of transport *H*
- Observations *y* at *n* stations

$$y_1 = H_{11}\, x_1 + H_{12}\, x_2 + \ldots + H_{1m}\, x_m$$

Concentration of [CO2]
Measured at station 1

Partial derivative of [CO2] at
station 1 regarding source 1

Source 1

Inverse problem = estimate x such that
(y = H x) + prior knowledge

Fundamentals of the Inversion Problem

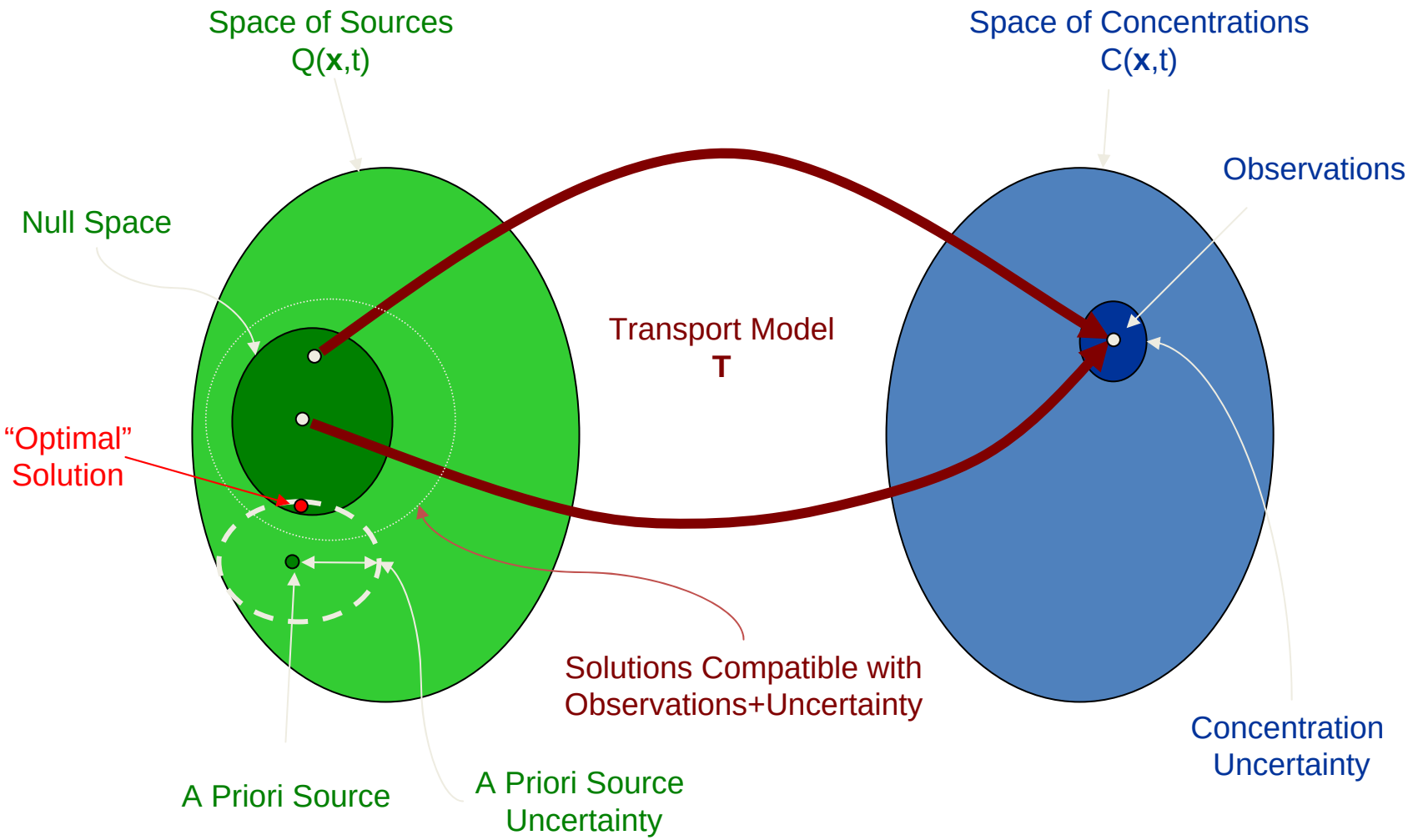

Atmospheric transport modeling

DIRECT APPROACH

$$Sc - \nabla \bullet (r C \vec{V}) = (r C) \frac{\partial}{\partial t}$$

• CO_2 Sources
Regional First guess
x_b ; *var/cov P*

Atmospheric transport
H

Simulated concentrations
y_{model}

Observations
y_o; *var/cov R*

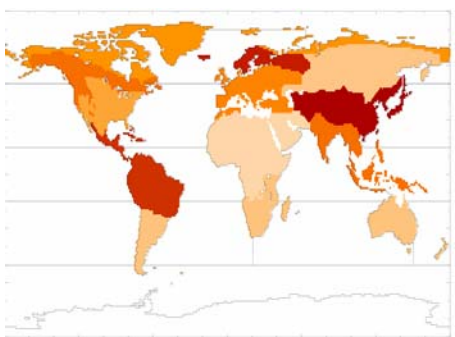

INVERSE APPROACH

$$H x = y$$

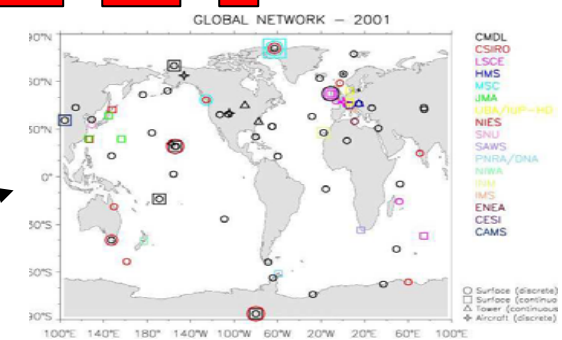

Estimation of x_a mimizing the distance between y_{model} and y_o

Estimate :

$$x_a = x_b + \left(H^T R^{-1} H + P^{-1}\right)^{-1} H^T R^{-1} (y_0 - H x_b)$$

Uncertainty :

$$P_a = (H^t R^{-1} H + P^{-1})^{-1}$$

See F Chevallier lecture

Small gradients

CO_2 field resulting from the release of 1 Pg C in boreal Eurasia

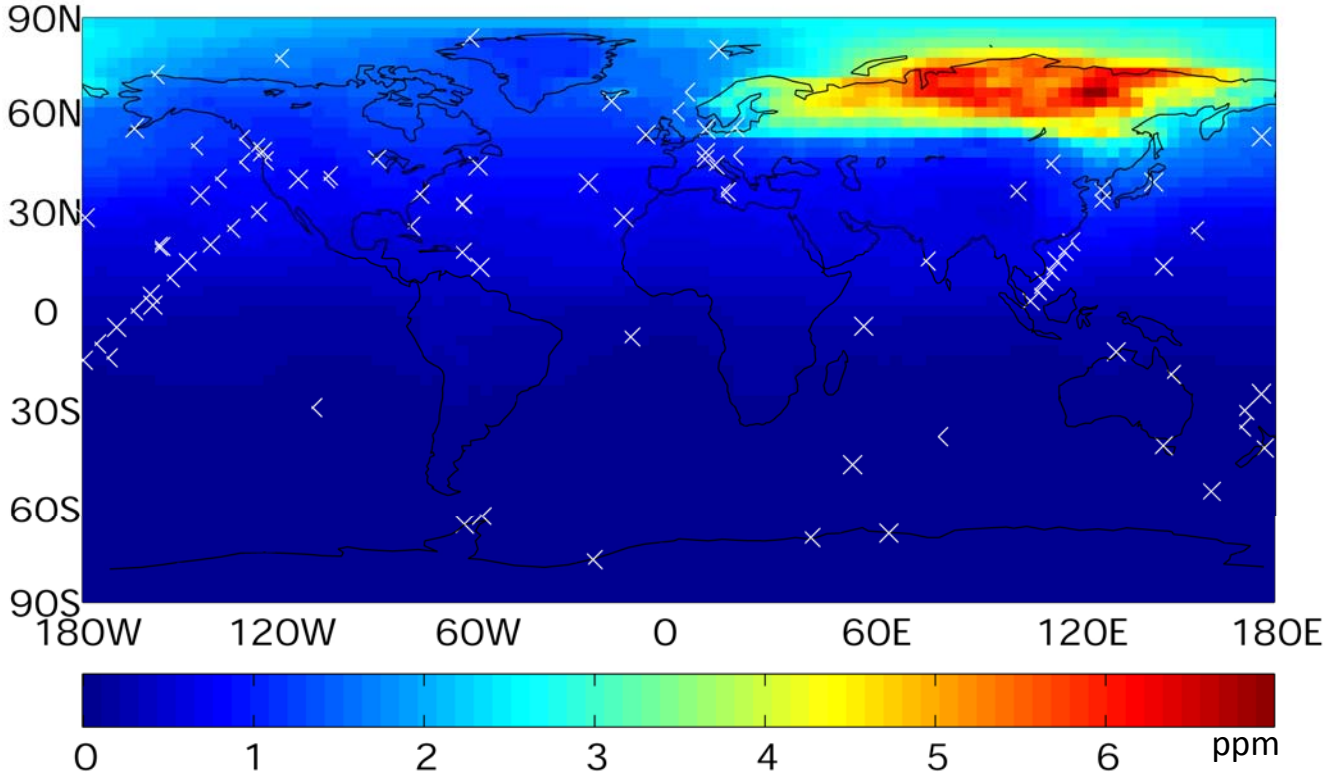

Time evolution of interhemispheric CO_2 gradient

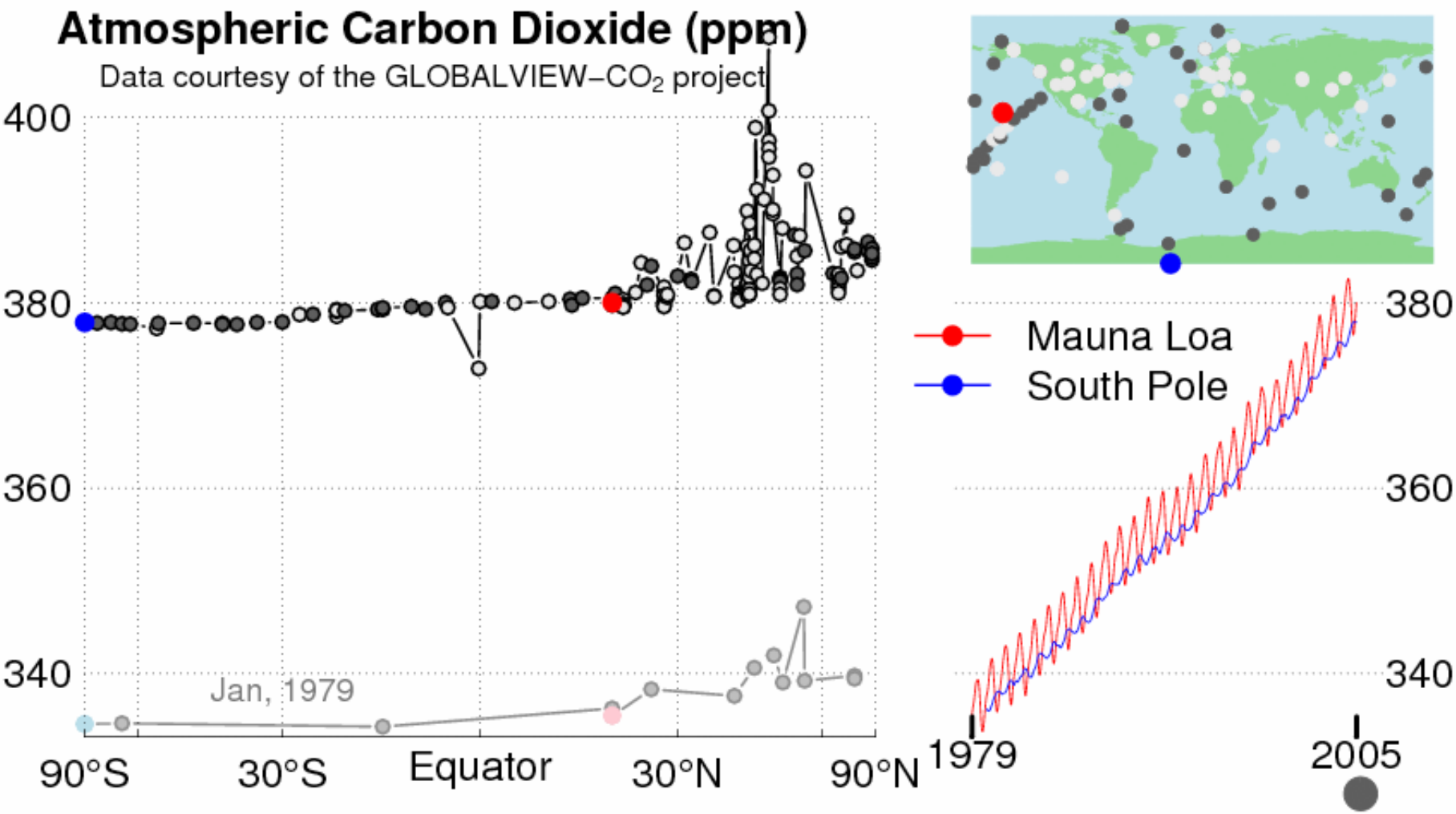

Global CO_2 field (500 m asl)

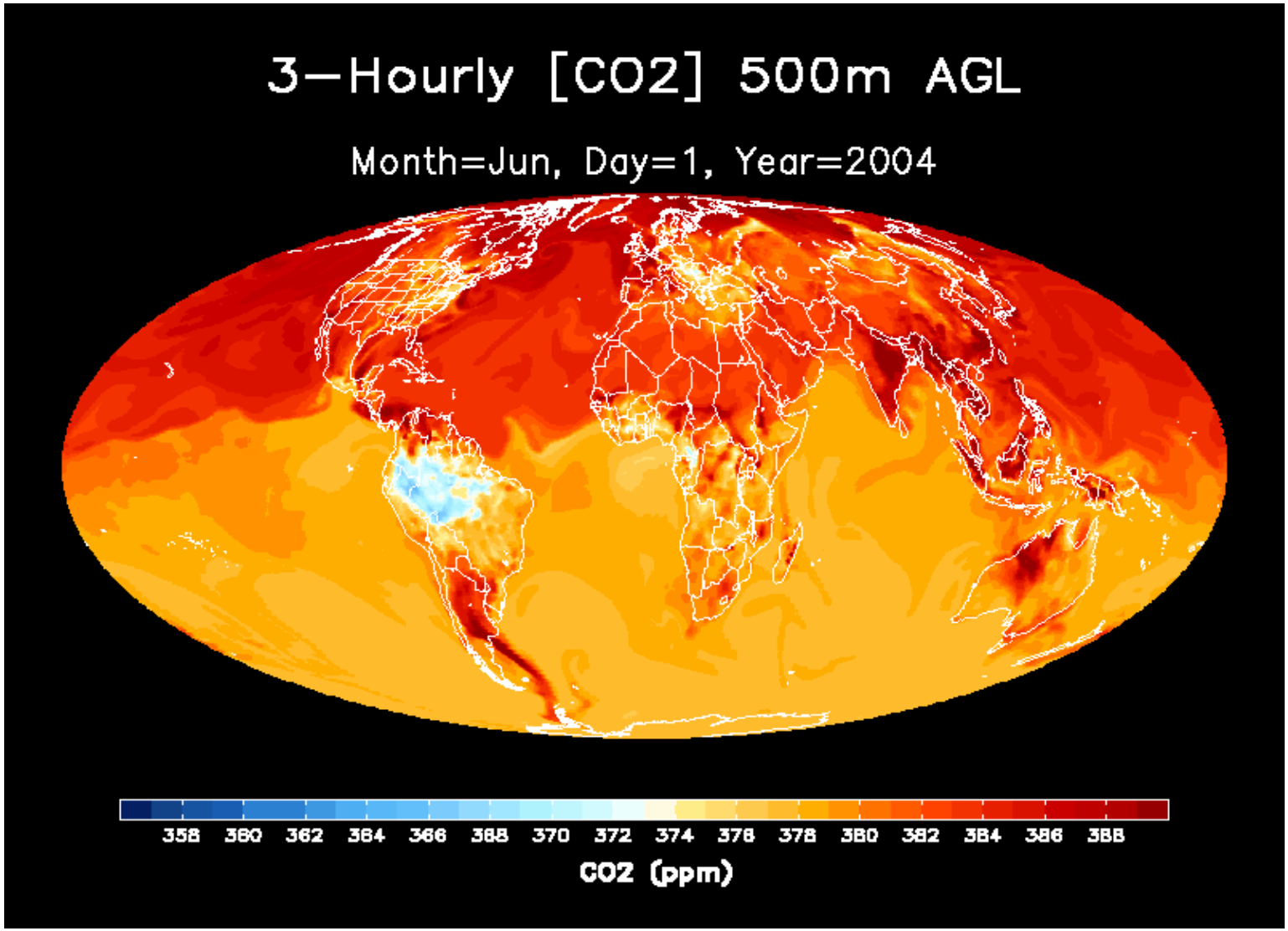

Zonal mixing >> meridional mixing => latitudinal gradients dominate the CO2 signal in the marine boundary layer

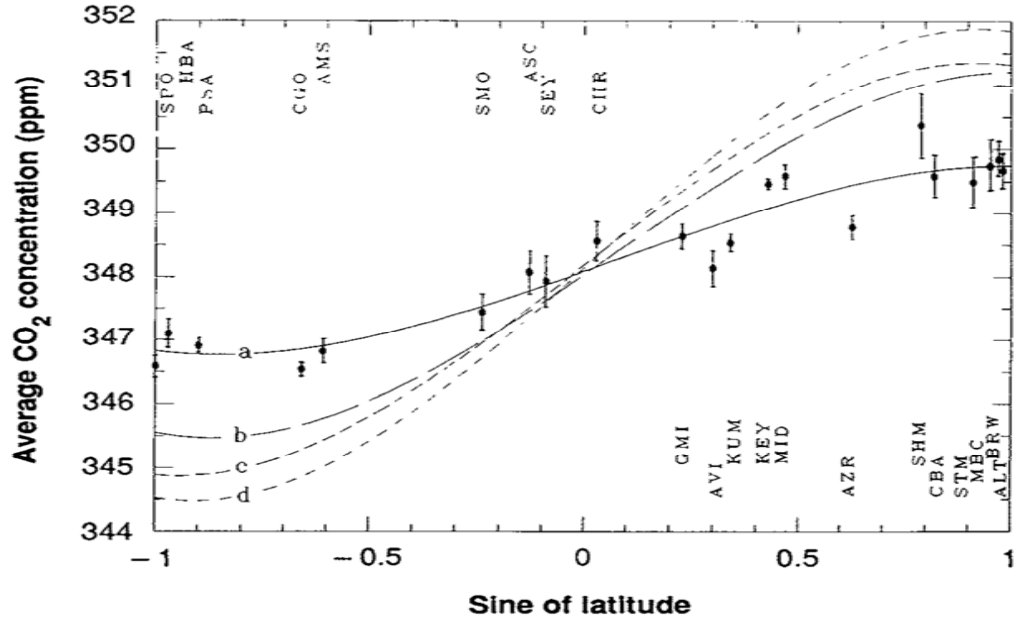

Fig. 1. Observed atmospheric CO_2 concentrations at the sites of the NOAA/GMCC flask network. The three-letter station codes are explained in Table 1. The error bars represent 1 SD of the annual averages at each site after adjustment to 1987. Curve (a) is a least-squares cubic polynomial fit to the data. The residual SD of the points with respect to the curve is 0.39 ppm. The concentration distributions at the NOAA/GMCC sites have also been calculated with the NASA/GISS GCM transport fields. Other curves are polynomial fits to the calculated CO_2 distributions (not shown) with fossil fuel emissions, seasonal vegetation (no net annual source or sink), tropical deforestation of 0.3 Gt of C per year, and three different cases of ocean uptake: (c), the compilation of CO_2 uptake based on the ΔpCO_2 data (Table 2) and our empirical transfer coefficients; (b), CO_2 uptake based on the same ΔpCO_2 map, but calculated with the Liss-Merlivat (*22*) relation for air-sea exchange; (d), an earlier estimate of ocean uptake (*21*) totaling 2.6 Gt of C per year.

Inter-hemispheric annual CO_2 gradient

Overestimated interhemispheric CO2 difference when ocean + fossil fuel emissions + balanced biosphere fluxes are modeled

$\Rightarrow$ Sink of CO_2 in northern hemisphere

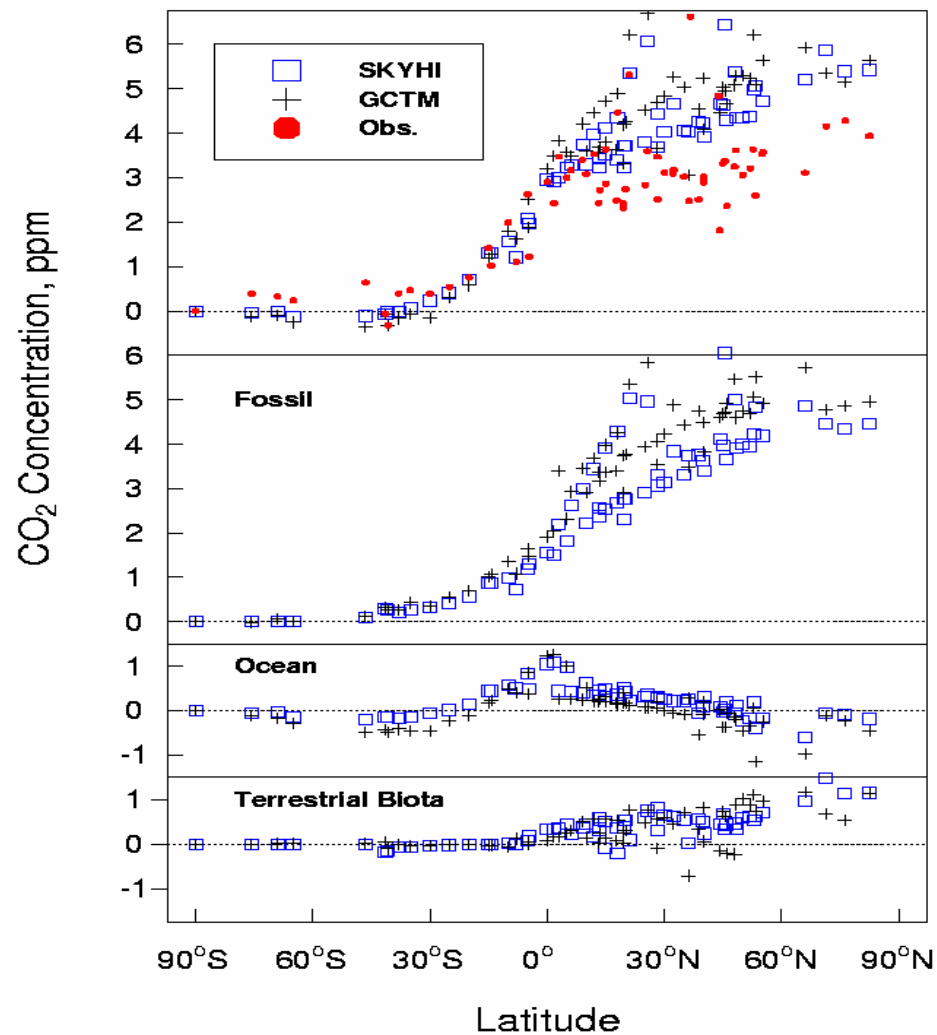

Large scale transport differences

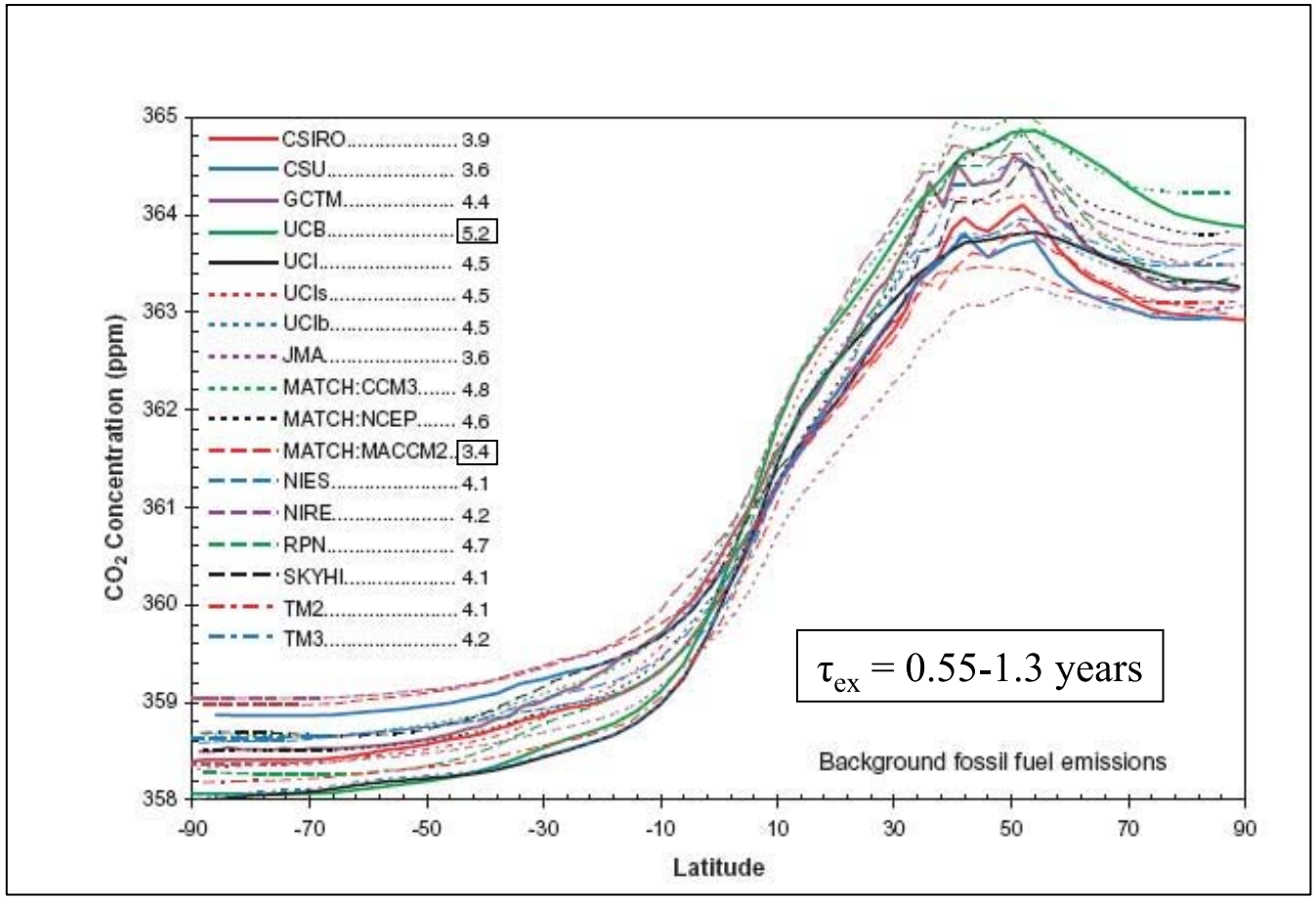

Gurney et al., Tellus B (2003)

Transcom 3 experiment (Gurney et al., 2002, *Nature*)

11 land regions, 11 ocean regions
15 transport models, same inverse procedure
Period 1992-1996

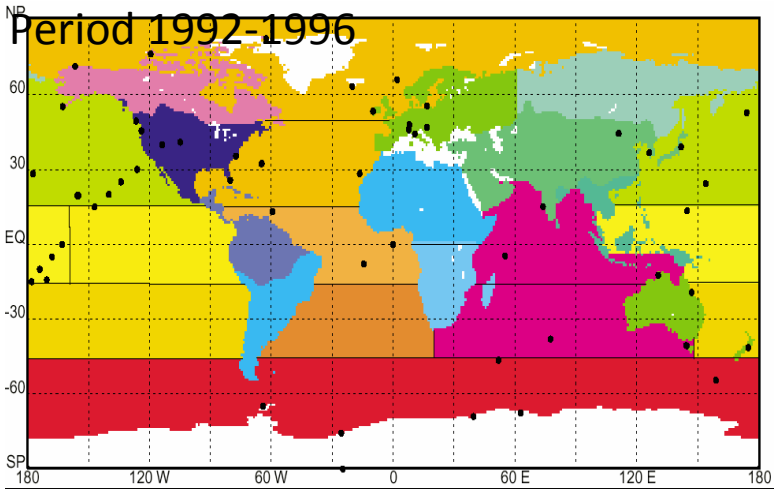

Latitudinal net fluxes
(fossil fuel subtracted)

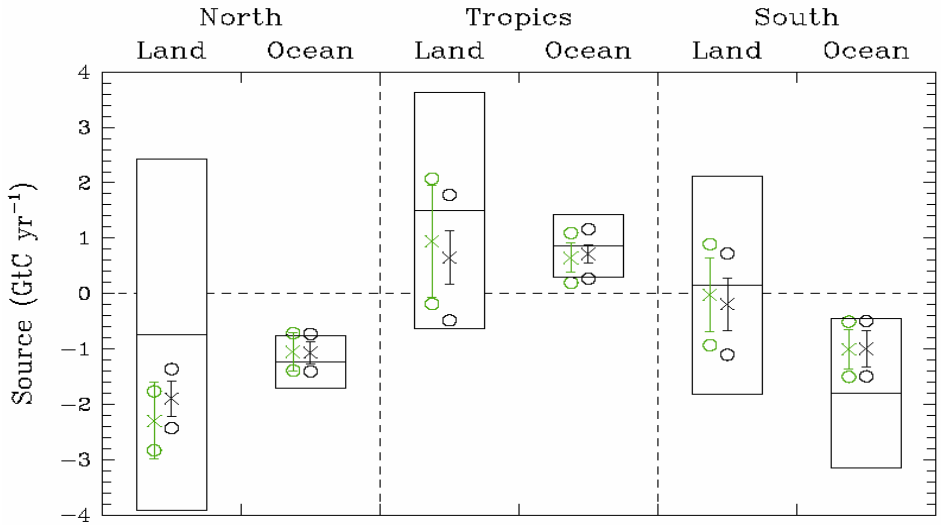

- Northern Hemisphere Land sink
- Reduction of southern oceans sink by 2 compared to Takahashi
- Deforestation is partly compensated by a tropical land uptake
- Effect of the seasonal rectifier over continents of the Northern hemisphere (Eurasia)

The mid 1990's : inversions of monthly CO2 data

Yearly flux estimates
Large regions

Monthly flux estimates
Large regions

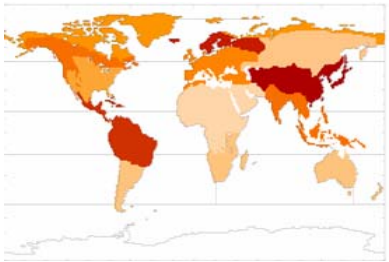

Transport model

Coarse global models

Global high resolution models, zoomable or regional models

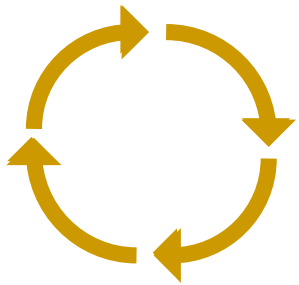

Surface fluxes

Atmospheric concentrations

Yearly observations
MBL & coastal sites

Monthly observations
MBL & coastal sites

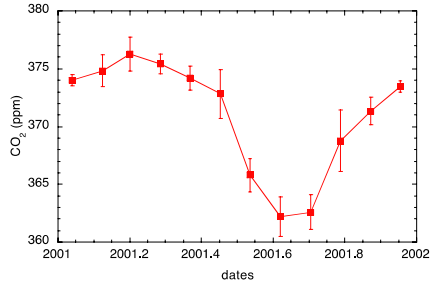

Monthly flux estimates
Model resolution or Small regions

Synoptic observations
All sites (continental)

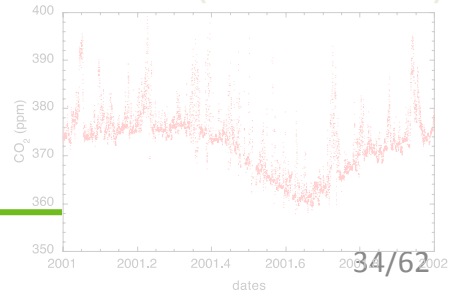

Inverse study by Peylin, Backer et al. (2002)

Sources \ Data	Annual [CO_2] (a)	Monthly [CO_2] (m)
Annual adjustment (TI)	*46 data* *n fluxes*	*46 * 12 data* *n fluxes*
Monthly adjustment (TD)	~~*46 data*~~ ~~*n * 12 fluxes*~~	*46 * 12 data* *n * 12 fluxes*

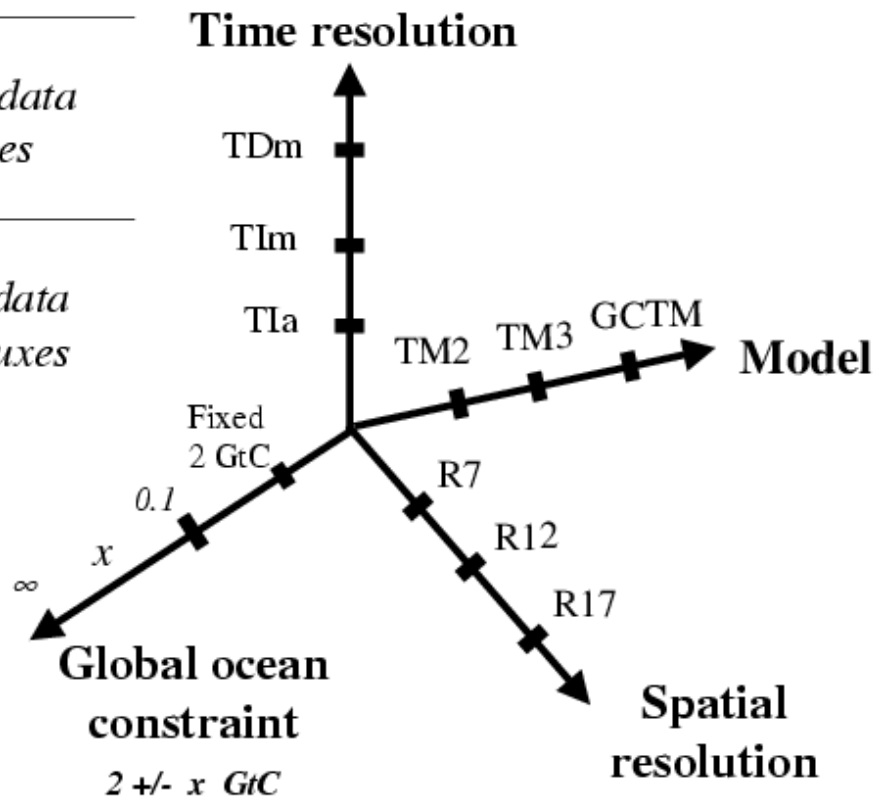

Seasonal rectifier effect

CO_2 gradients resulting from transport applied to seasonally balanced biospheric fluxes

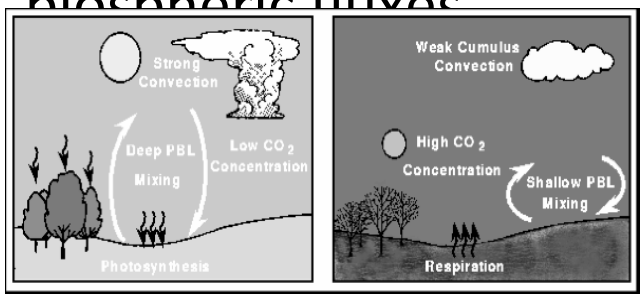

summer winter

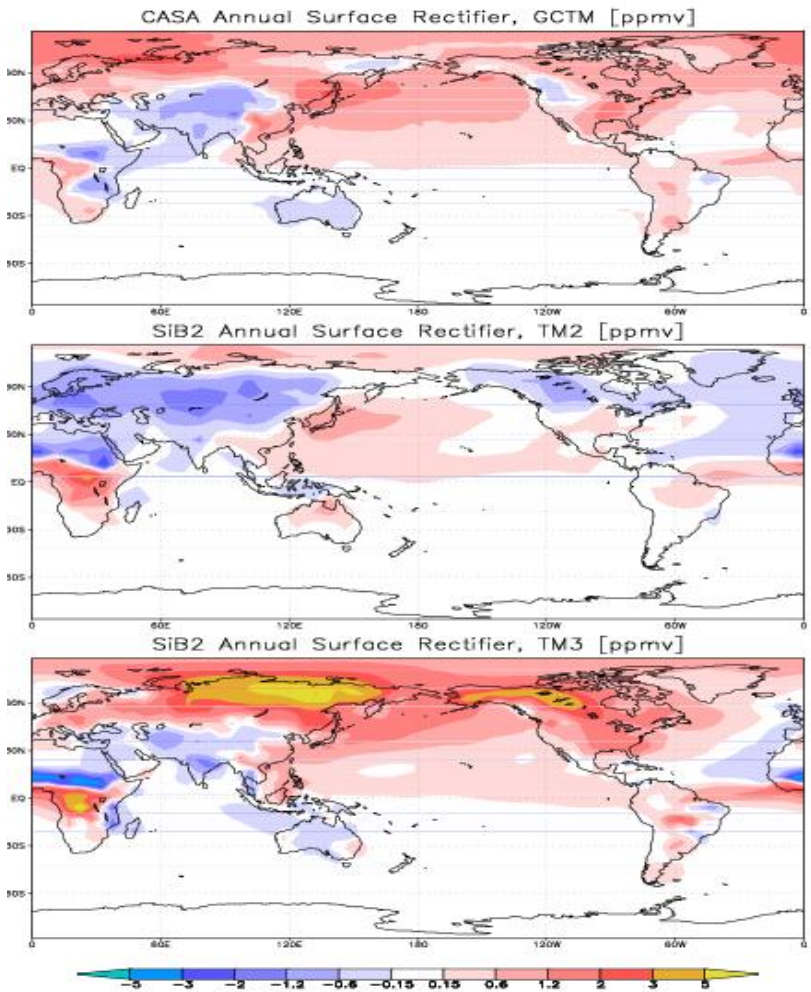

The rectifier effect is reflected in the surface network gradients but also in the vertical structure of CO2

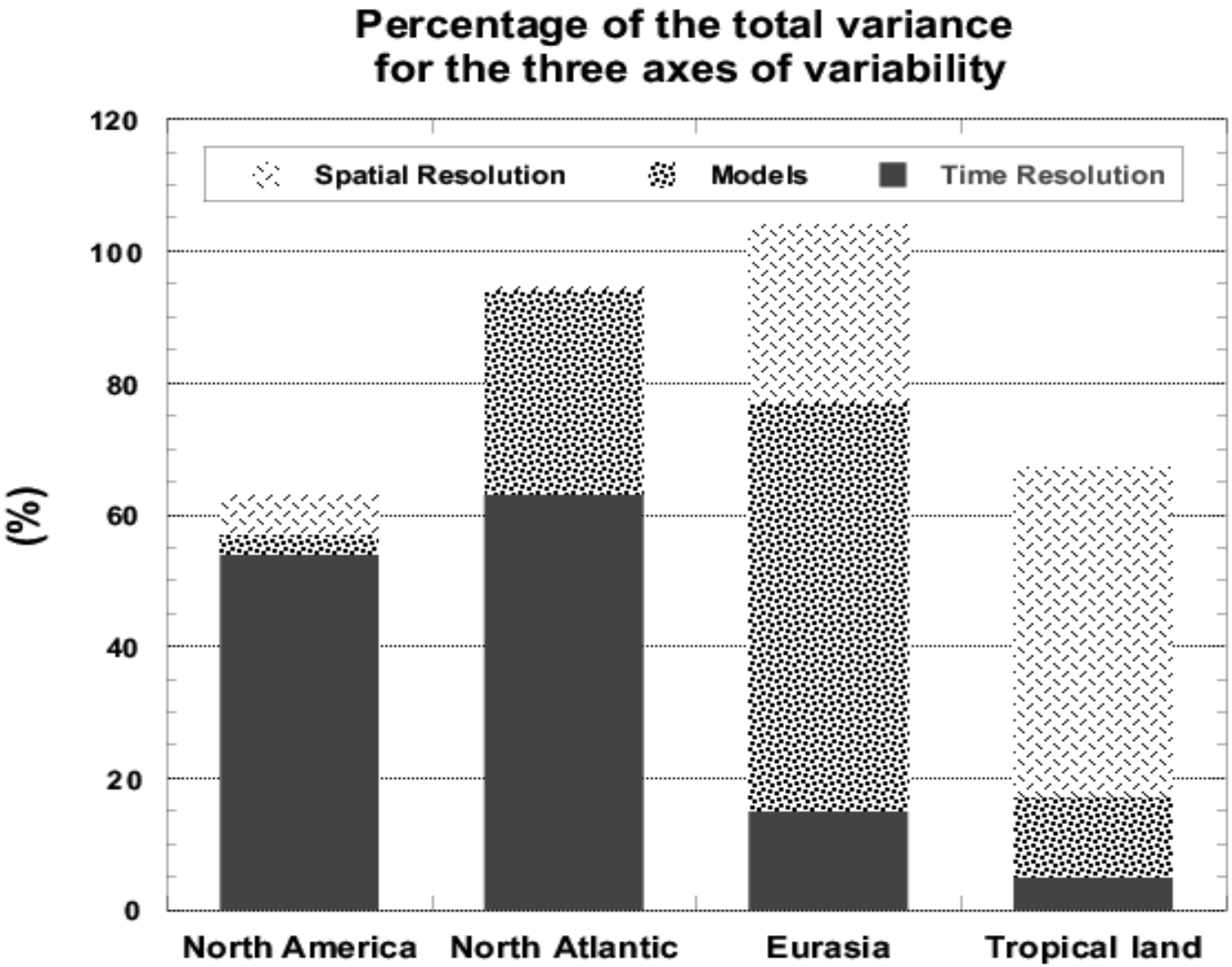

Peylin, Backer et al. (2002)

Rectifier evaluation using vertical CO_2 profiles

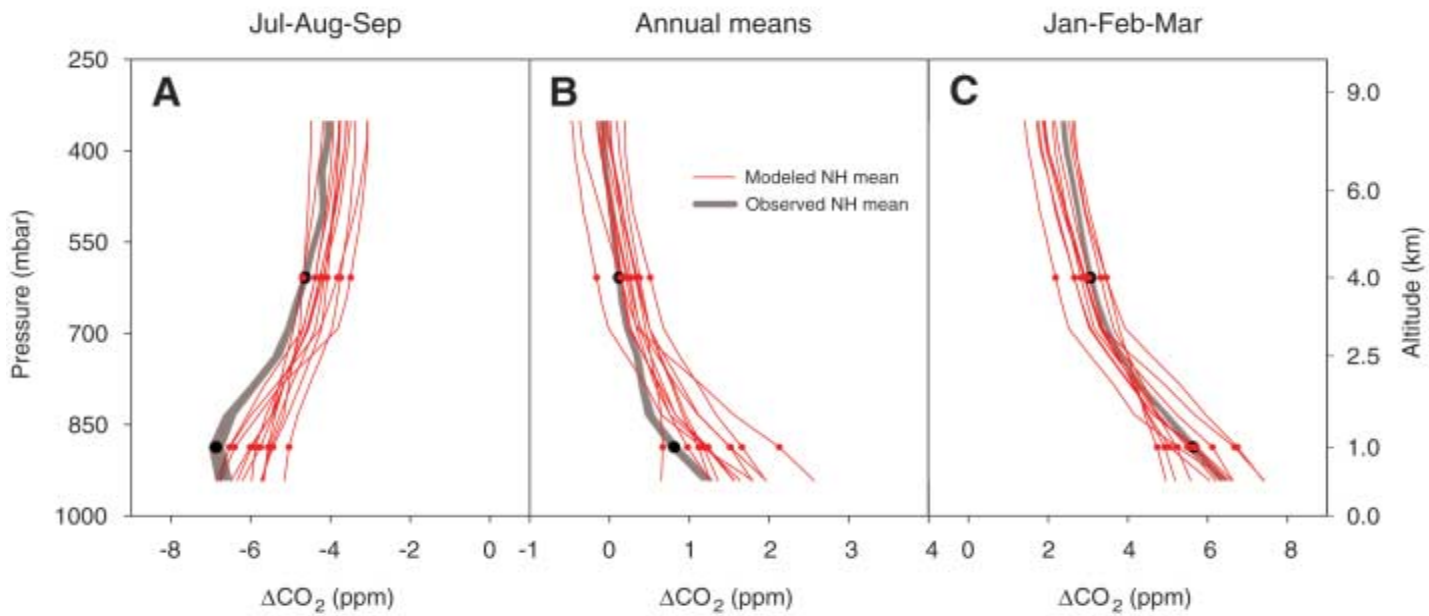

Fig. 2. (**A** to **C**) Observed Northern Hemisphere average profiles compared with predictions of the 12 T3L2 models over the same seasonal intervals as in Fig. 1. Gray lines indicate the observed average vertical CO_2 gradients (center) and uncertainties (width) from Fig. 1 (*25*). The model output was processed in the same way as the observations at each site before averaging (*25*). Symbols indicate 1- and 4-km values used for calculating the vertical gradients shown in Fig. 3. The horizontal axis in (B) is zoomed by a factor of 2 relative to those in (A) and (C).

Correlation between inverted Northern and Tropical land sink

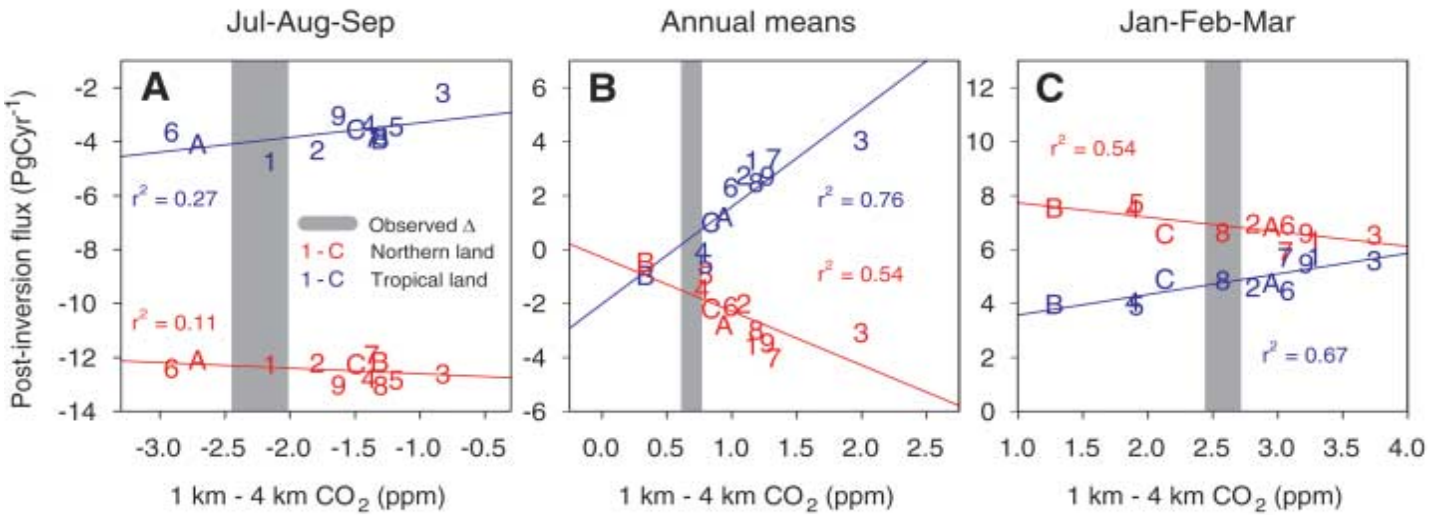

Fig. 3. Northern land and tropical land carbon fluxes for the 1992 to 1996 time period estimated by the 12 T3L2 models plotted as a function of the models' post-inversion predicted mean vertical CO_2 gradients for the same seasonal intervals as Fig. 1. The vertical axis in each plot represents the estimated fluxes for all northern land regions (red) and all tropical-land regions (blue) averaged over Northern Hemisphere summer (**A**), all months (**B**), and Northern Hemisphere winter (**C**). The horizontal axis represents the predicted Northern Hemisphere vertical CO_2 difference between 1- and 4-km altitude at these same times. The plotted numbers (1 to 9) and letters (A to C) correspond to the 12 models listed in table S2. Gray bars indicate the observed vertical CO_2 differences (center) from Fig. 2 and uncertainties (width) (*25*). The lines in each plot are linear least-squares fits to the modeled values.

Models compatible with vertical profiles estimate weaker tropical source (0.1 Pg C y-1) and a weaker northern sink 1.5 Pg C y-1, instead of 1.8 – 2.4 Pg C y-1 in former studies

Interannual variations (IAV) of global fluxes

Global scale

- Bousquet et al. (2000)
- Rayner et al. (2001.)

- LPJ model (Sitch et al.)
- SLAVE model (Friedlingstein)
- OPA model (Le Quéré et al.)

Land component dominates IAV

Tropical IAV is larger than NH IAV

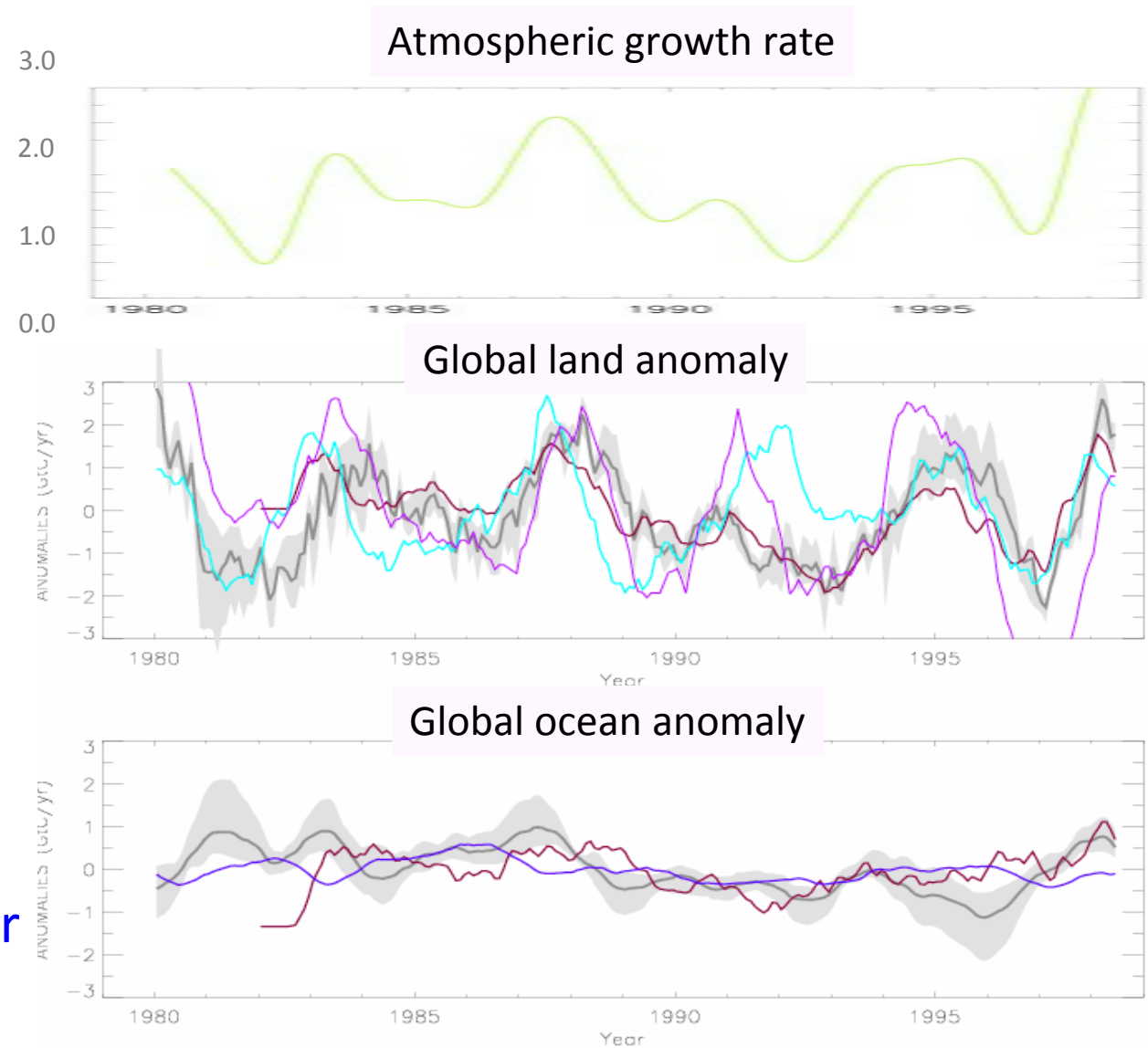

IAV from 13 inversions

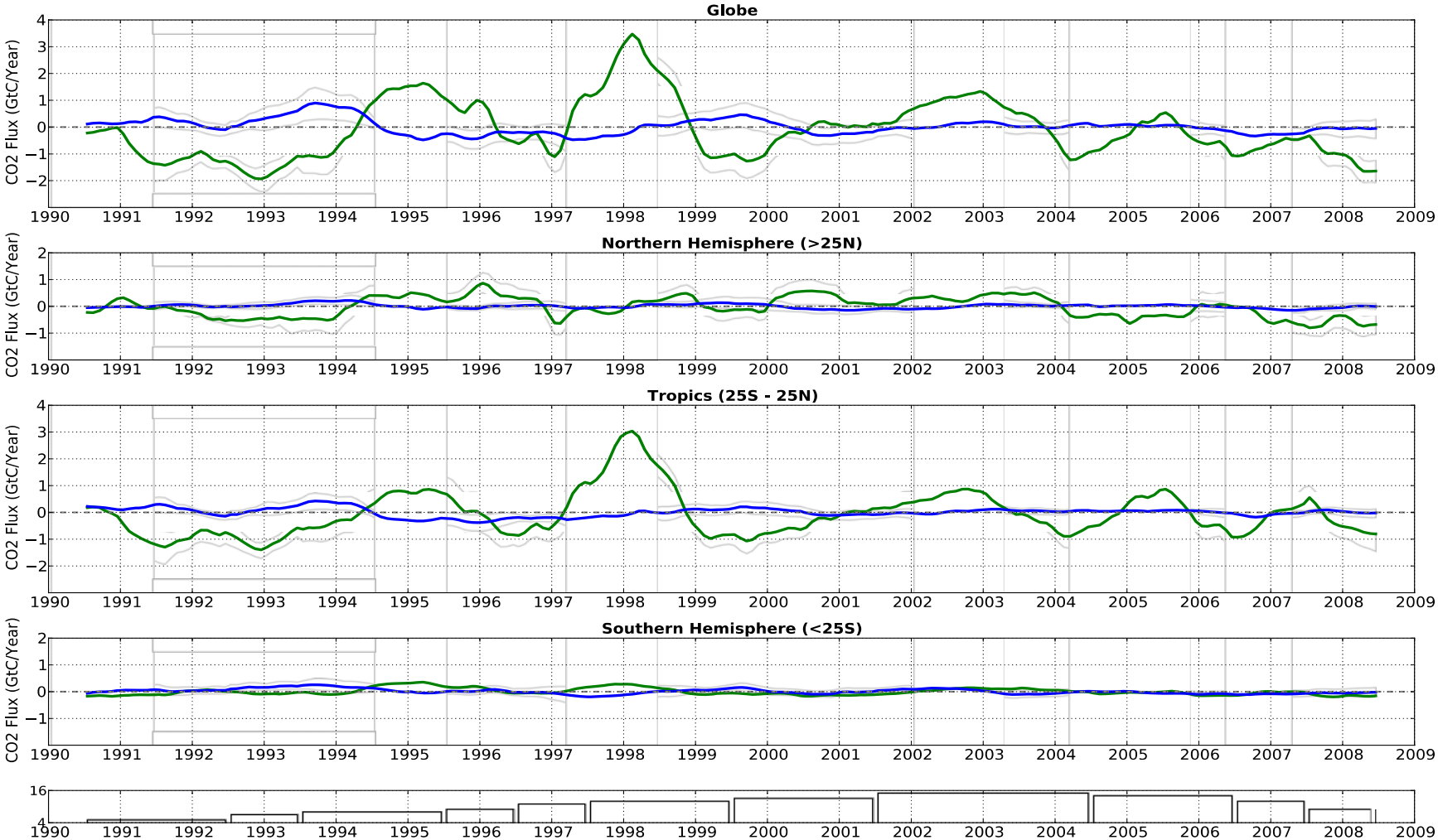

Interannual variations of regional fluxes

Regional scale : Equatorial Pacific

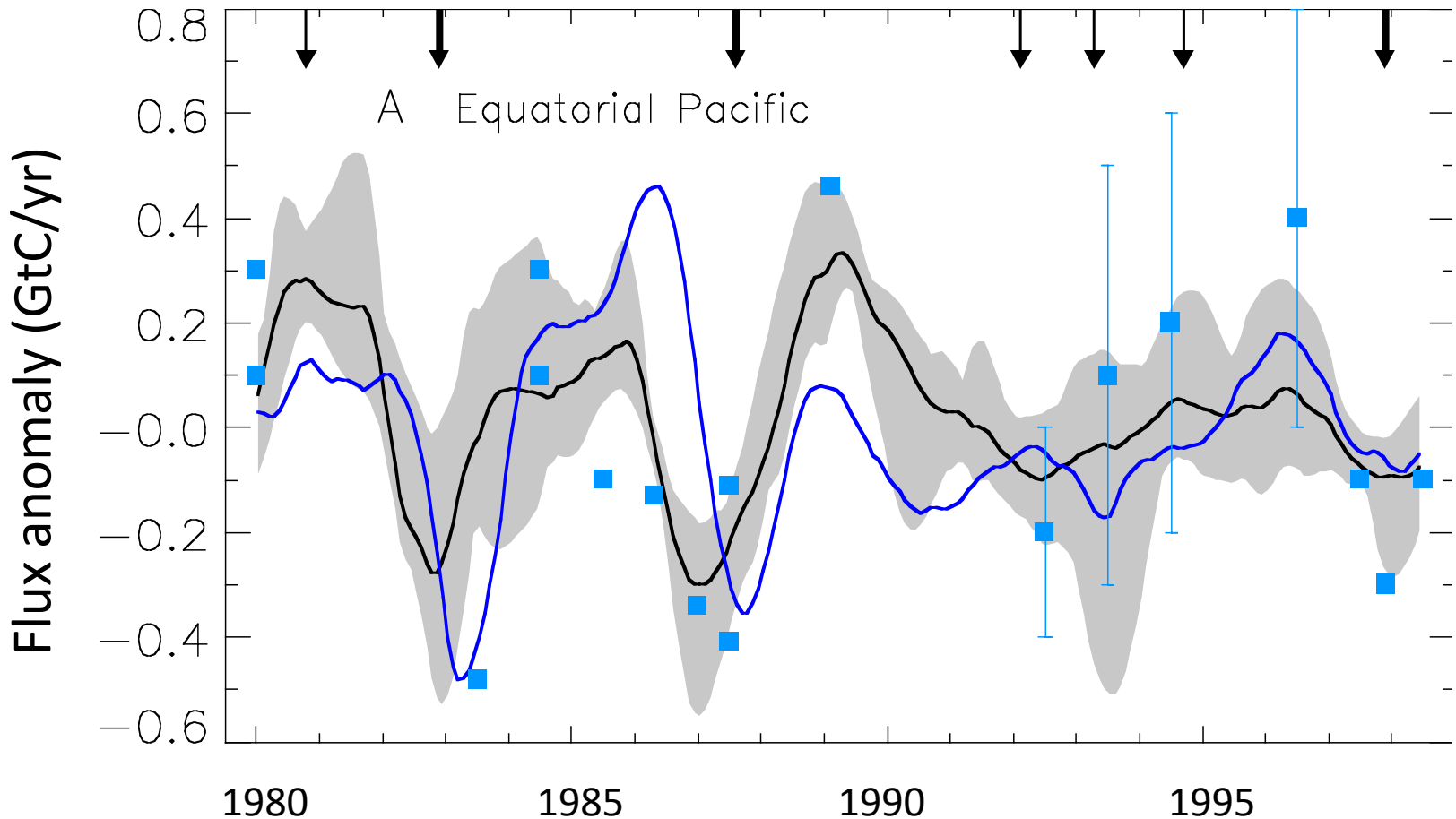

Inversion results over Europe : Comparison with biogeochemical models

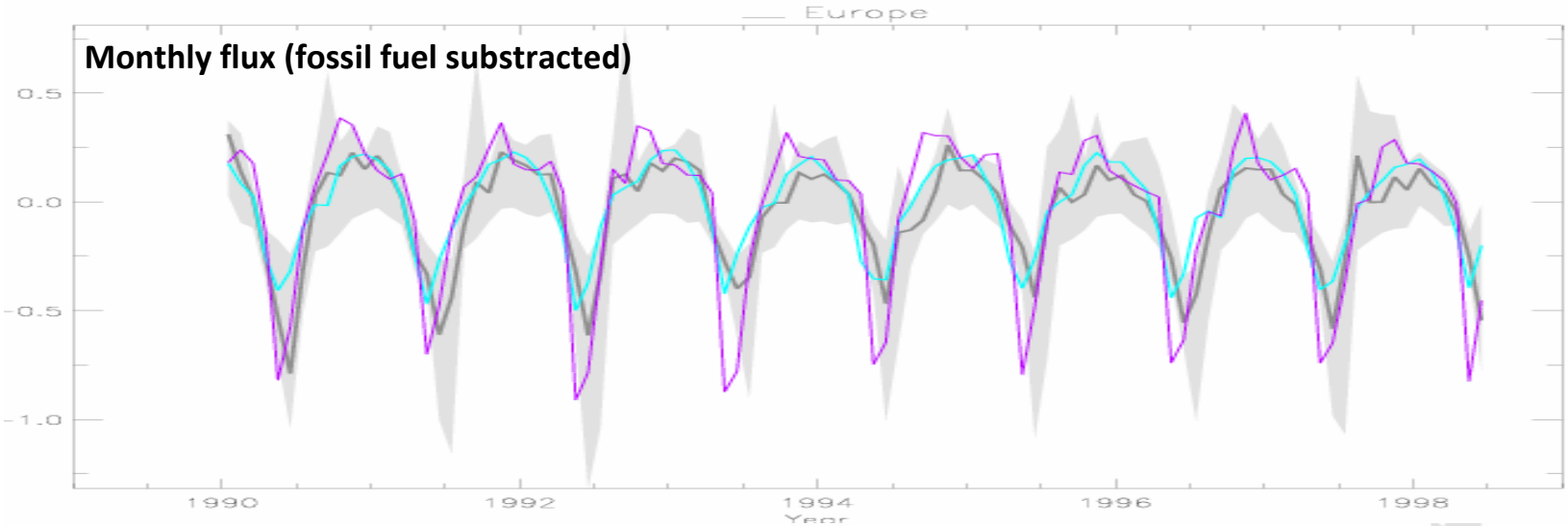

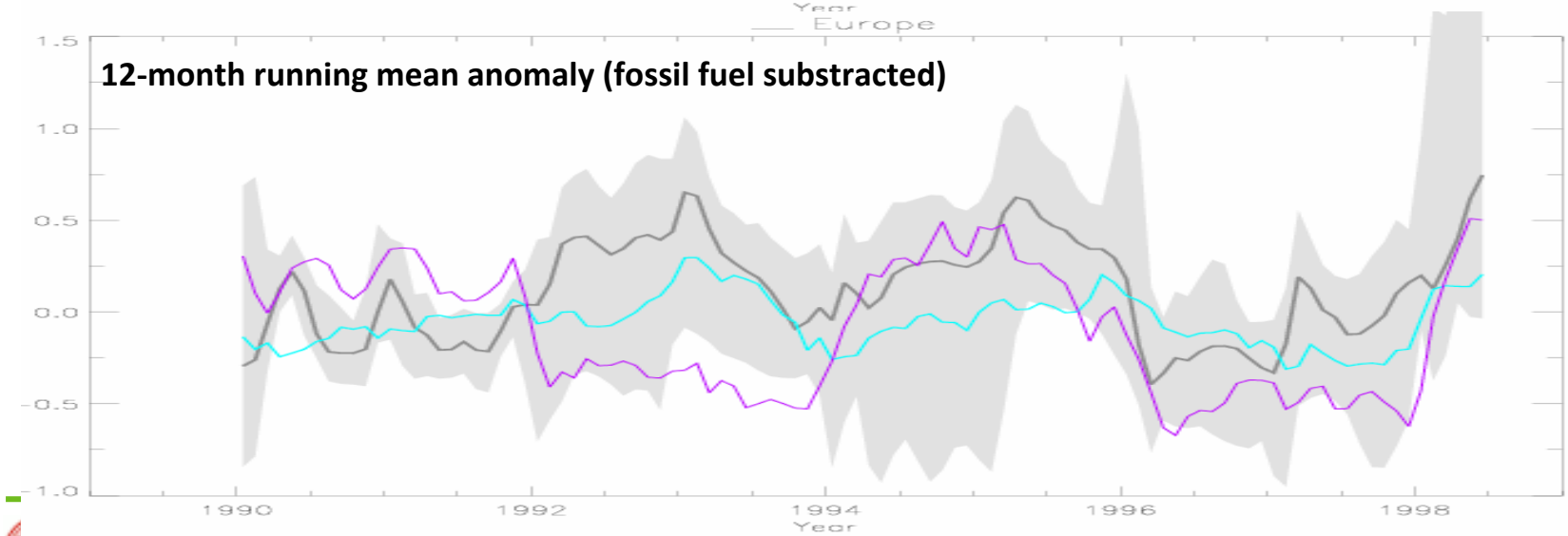

Inversion (Bousquet et al.) LPJ model (Sitch et al.) SLAVE model (Friedlingstein et al.)

Resolution of inversions (high resolution)

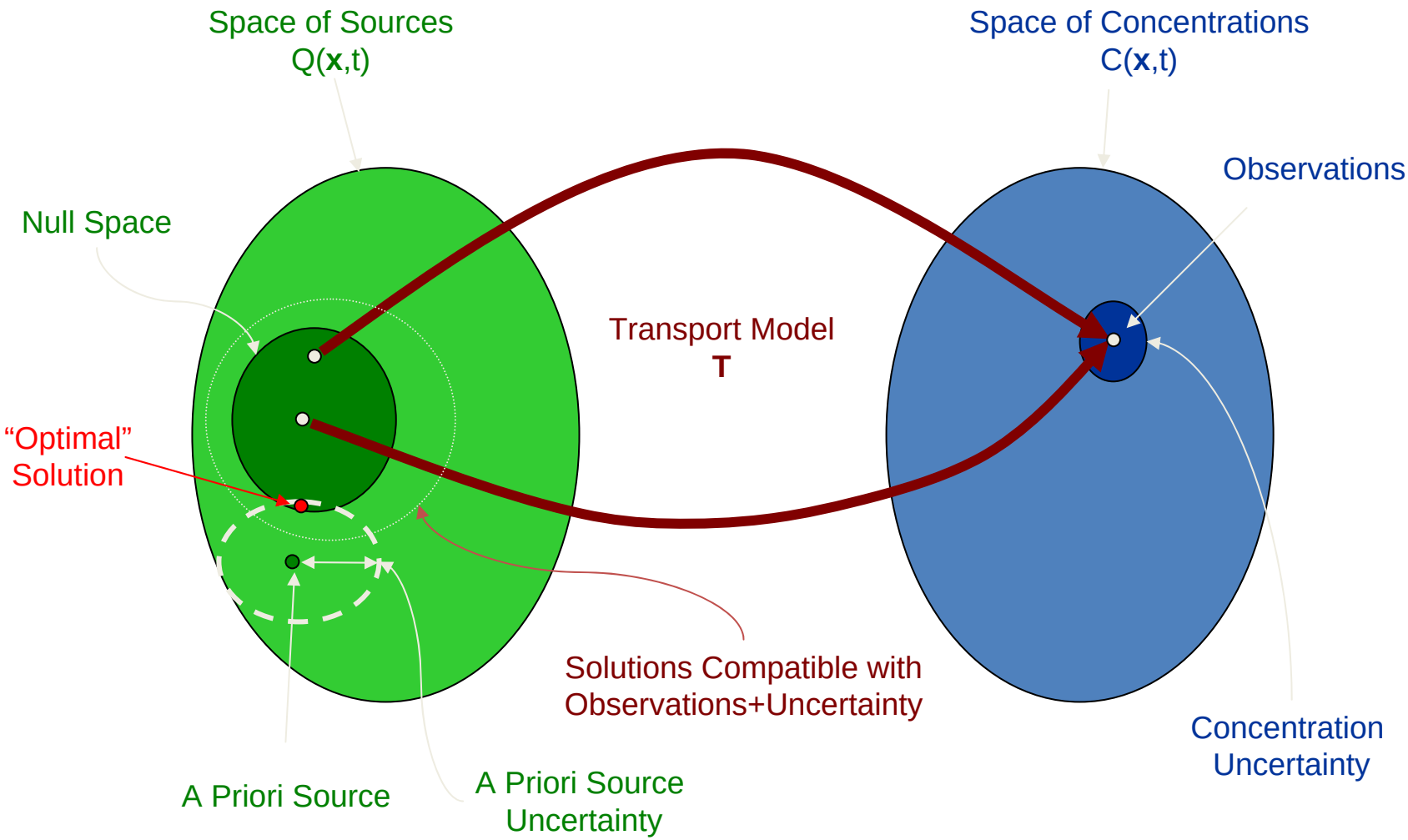

Coarse resolution

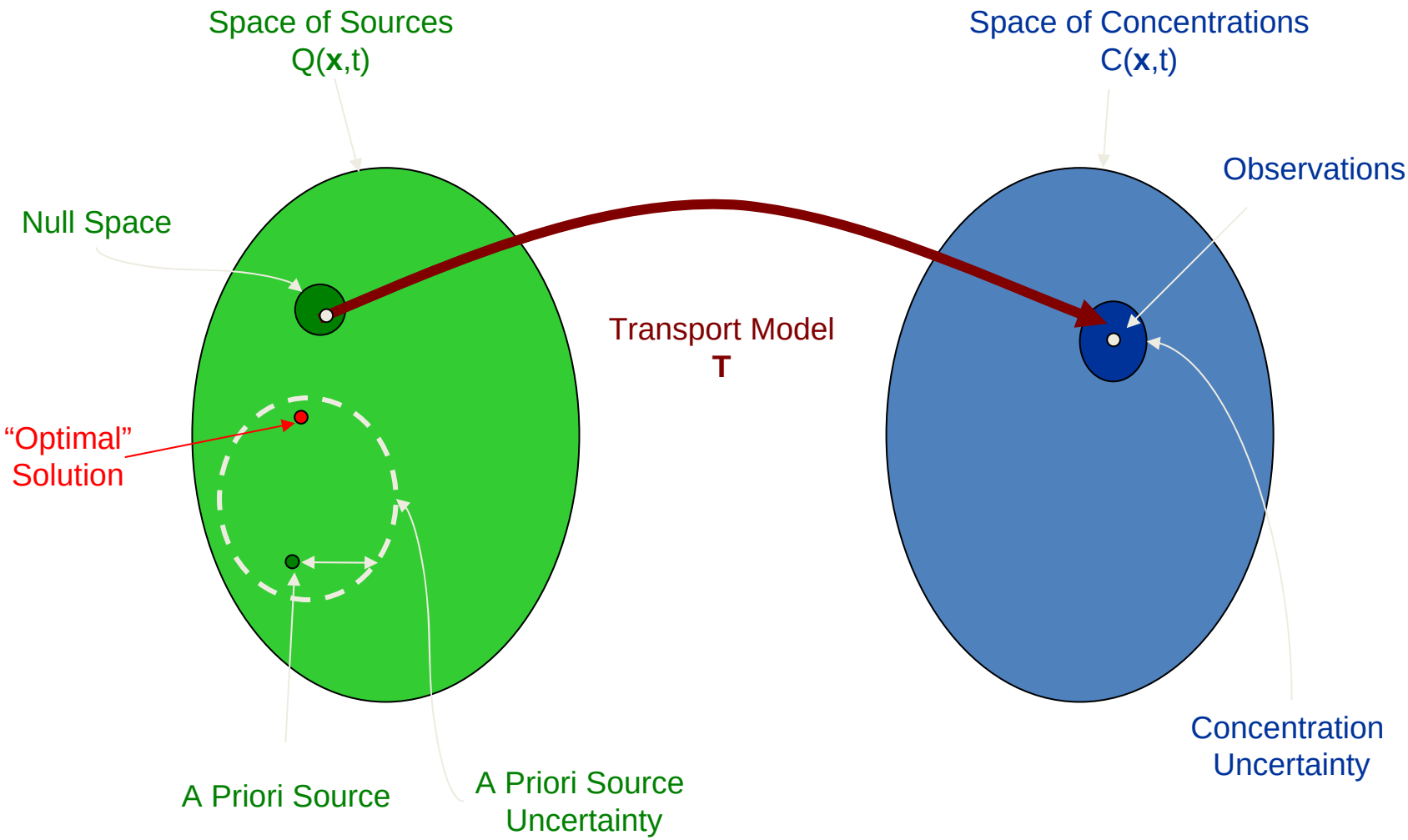

Large regions vs. model resolution inversion

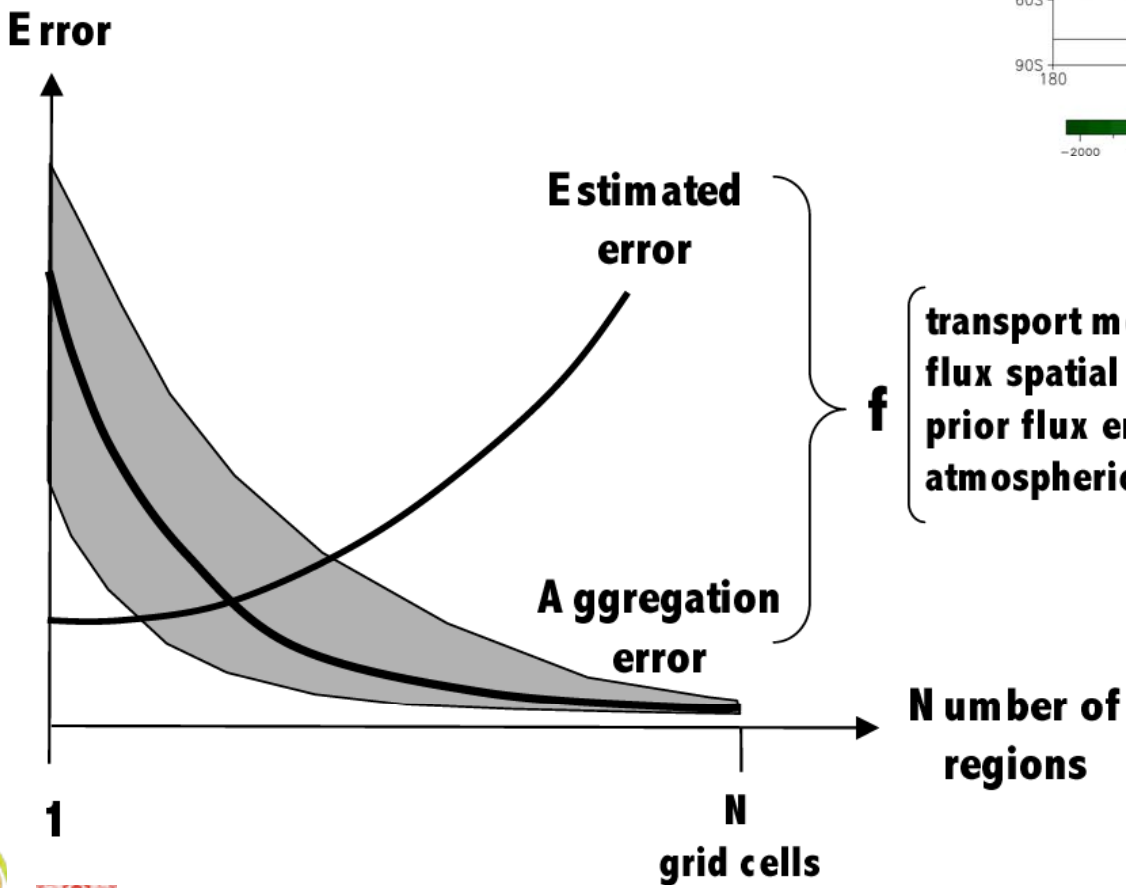

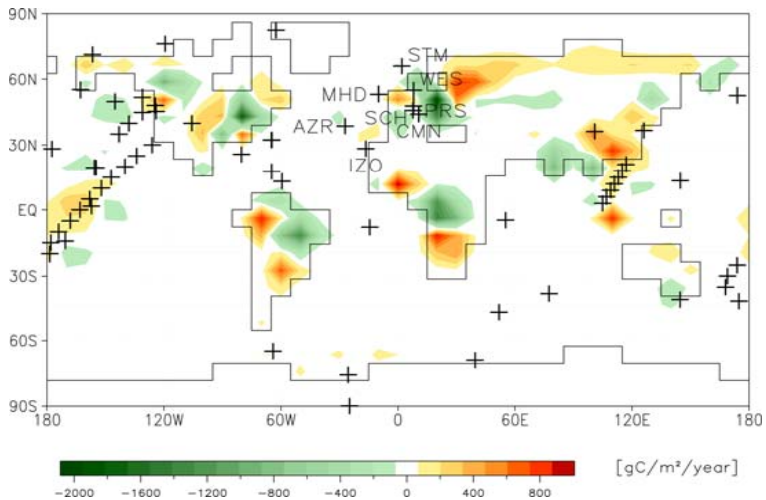

A 2GtC/yr Sink over Europe, consistent with the GLOBALVIEW Network Observations

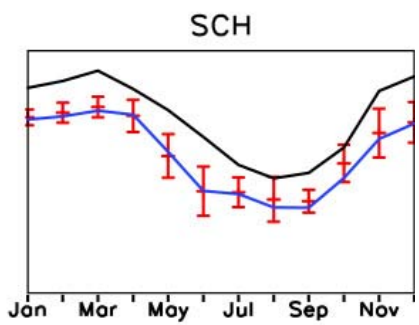

Heimann et Kaminski, 2001
Peylin et al., 2001

The mid 2000's : inversions at model grid resolution

See presentation by F Chevallier

Yearly flux estimates
Large regions

Monthly flux estimates
Large regions

Transport model

Regional mesoscale model

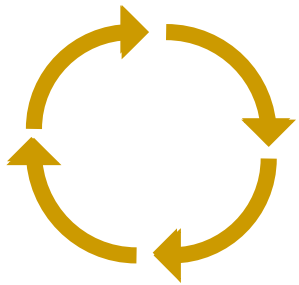

Surface fluxes

Atmospheric concentrations

Yearly observations
MBL & coastal sites

Monthly observations
MBL & coastal sites

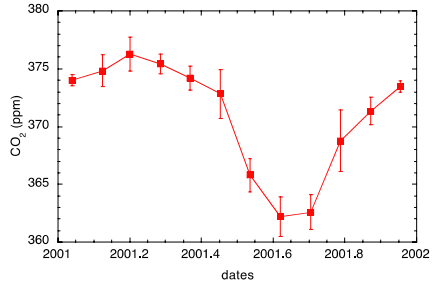

Hourly to daily flux estimates

Model grid resolution

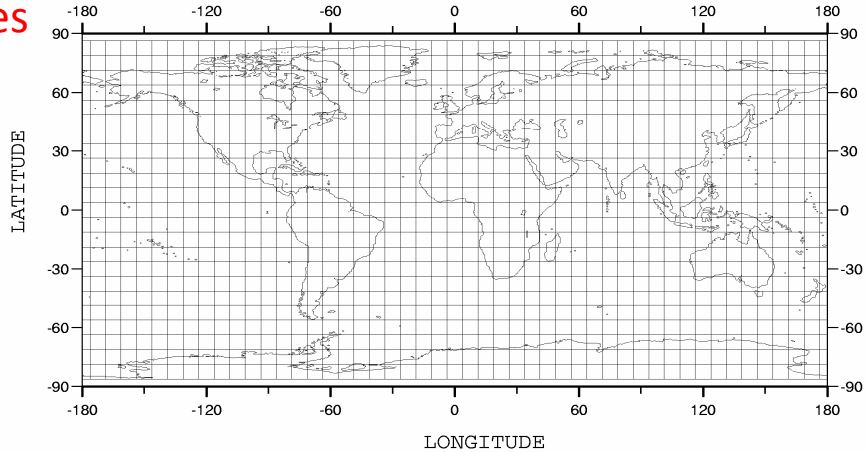

Synoptic observations
All sites (continental)

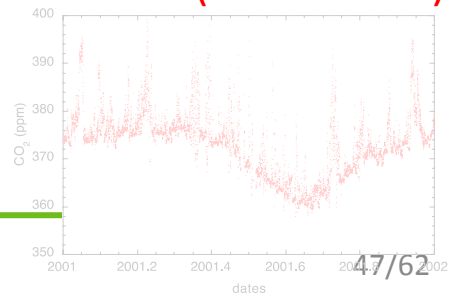

1 - Atmospheric measurements

2 - Data Integration in models

3 - Towards regional estimates

Diurnal rectification effects at continental sites

Near surface accumulation of respired CO2 followed by dilution of CO2 uptake by daytime convection (boundary layer mixing or deep convection in the Tropics)

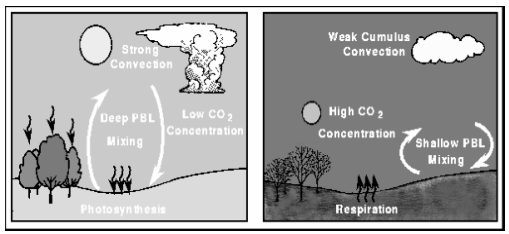

Day Night

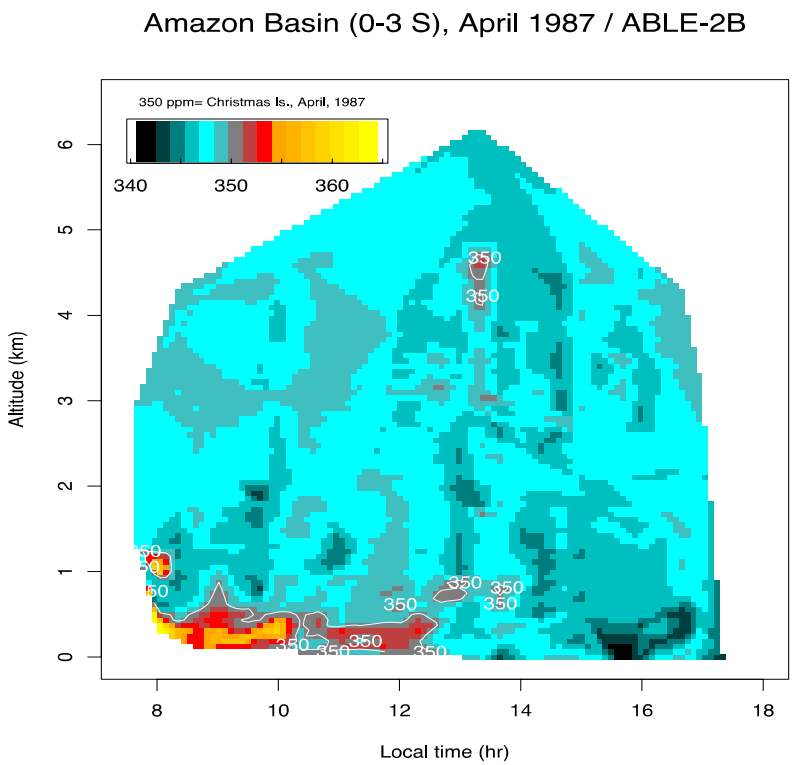

Figure II-8. Time-height cross section of CO_2 concentrations during ABLE2B, from 15 flights in the central Amazon Basin (0-3 S latitude) in April 1987. Note the development of the CO_2-rich PBL, with low concentrations aloft. In late afternoon the low values develop in the PBL when it is at its maximum thickness; these low values are supplied by the rectification process to the higher altitudes and adjacent oceans (Wofsy and Harriss, 1987, unpublished [available at ftp:// ftp-gte.larc.nasa.gov]).

REMO Model Vertical cross section of CO2

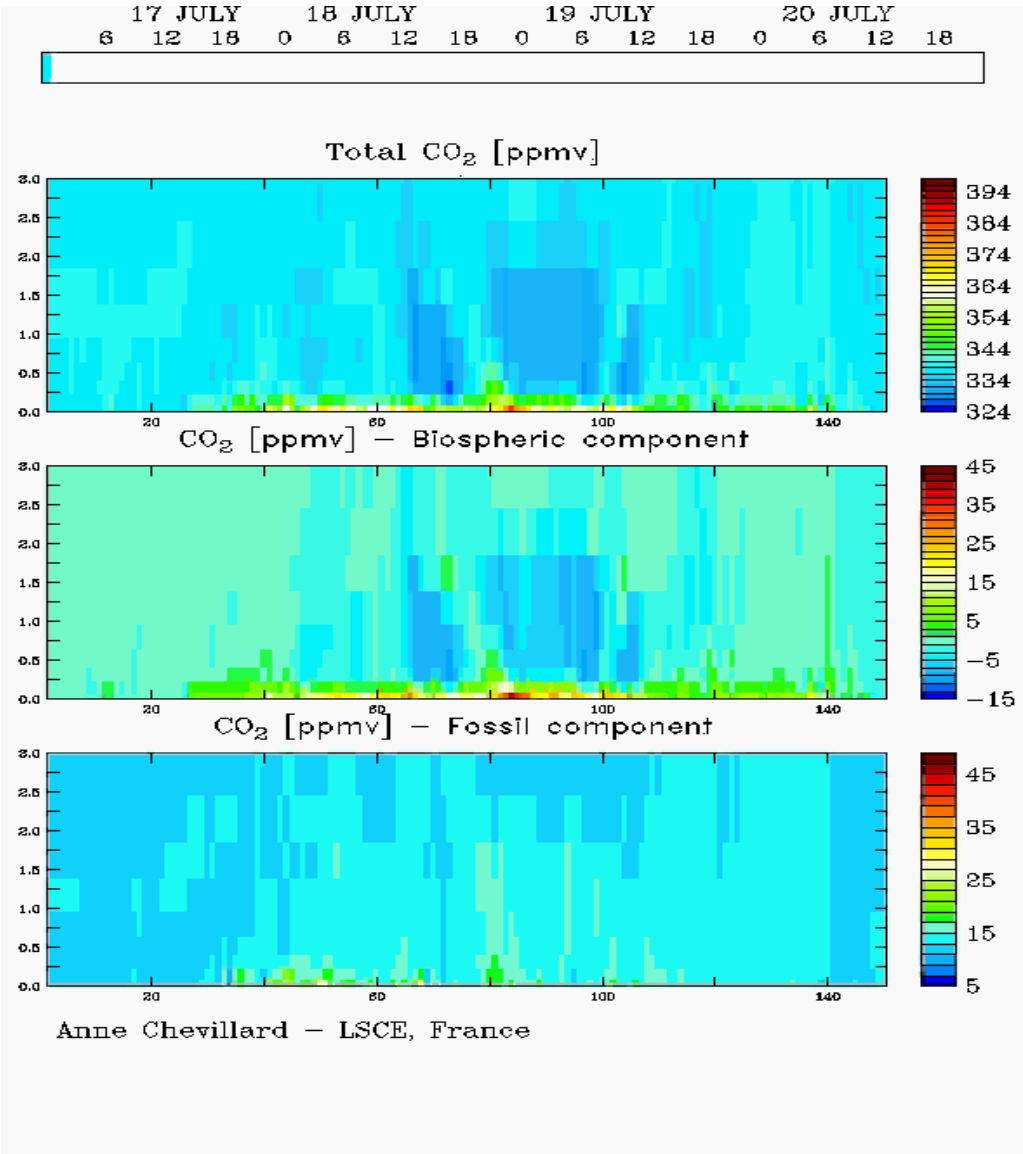

REMO Model Horizontal cross section of CO2

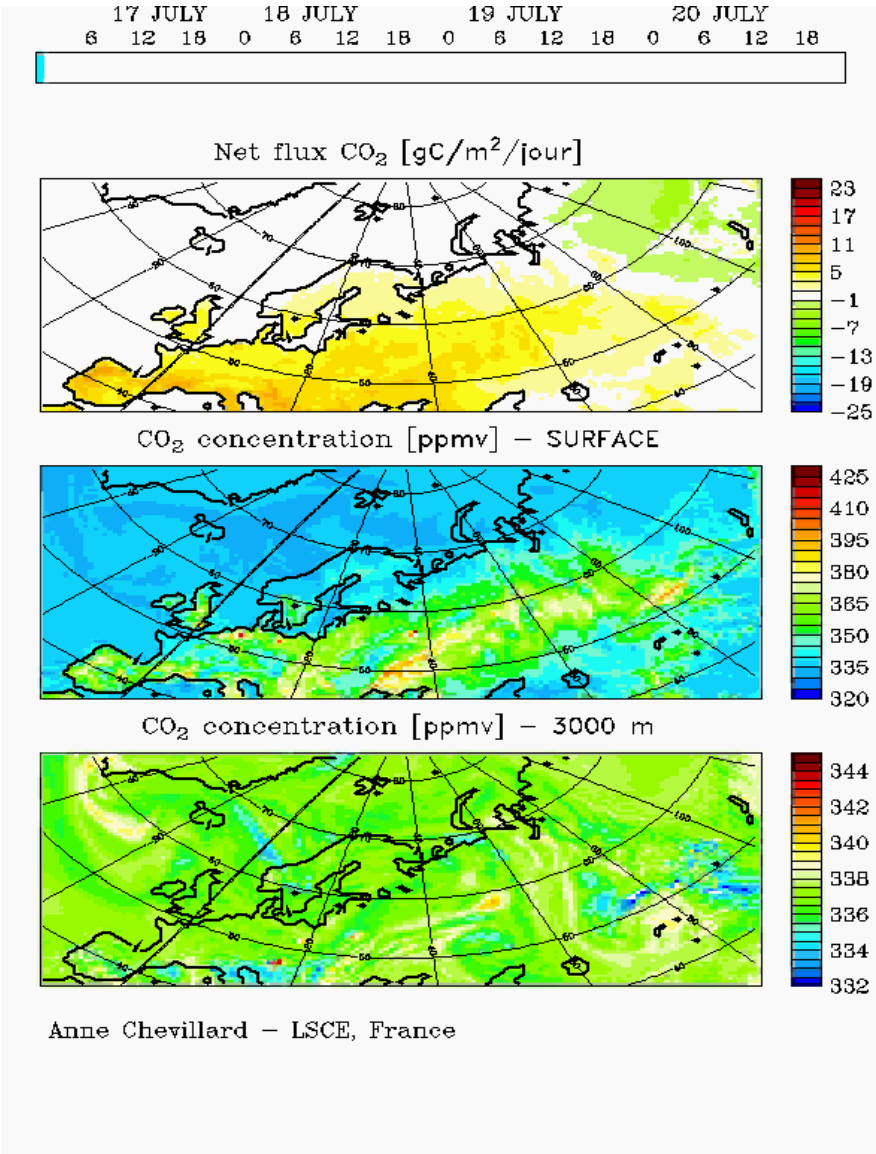

- Fluxes

- Surface CO2

- 3000 m CO2

Continental signals and transport errors

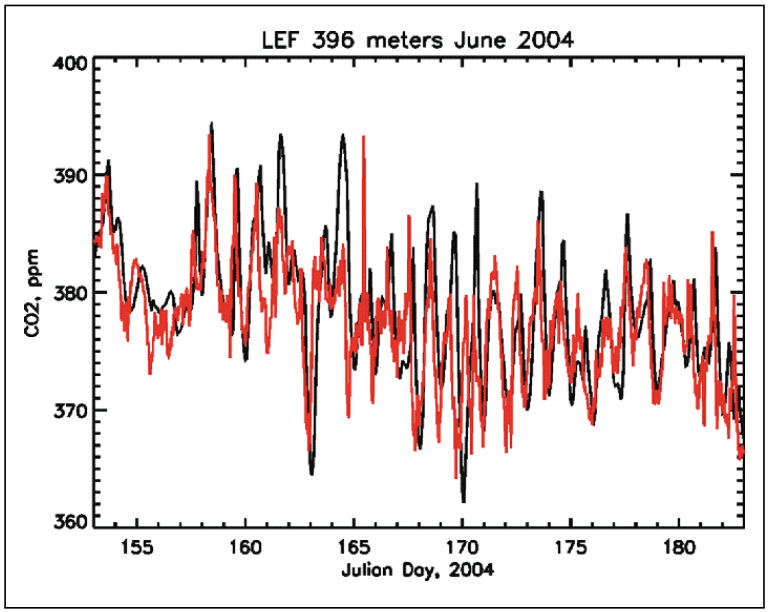

Same carbon fluxes (optimized CarbonTracker) transported by TM5 and WRF-STILT

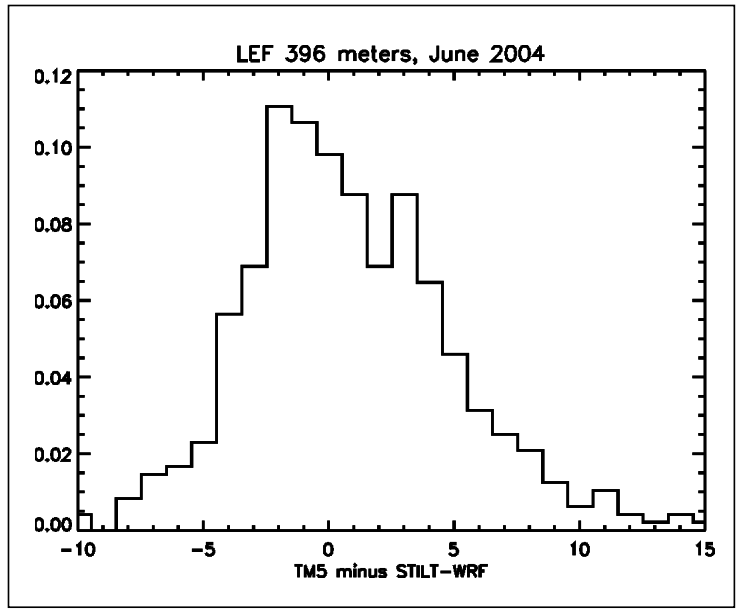

Mean difference = 1.2 ppm
Standard deviation = 4.5 ppm

Comparable to uncertainty
from using different carbon flux models
run with the same meterology

Total CO_2 at ground level

forward modelling (July 1998)

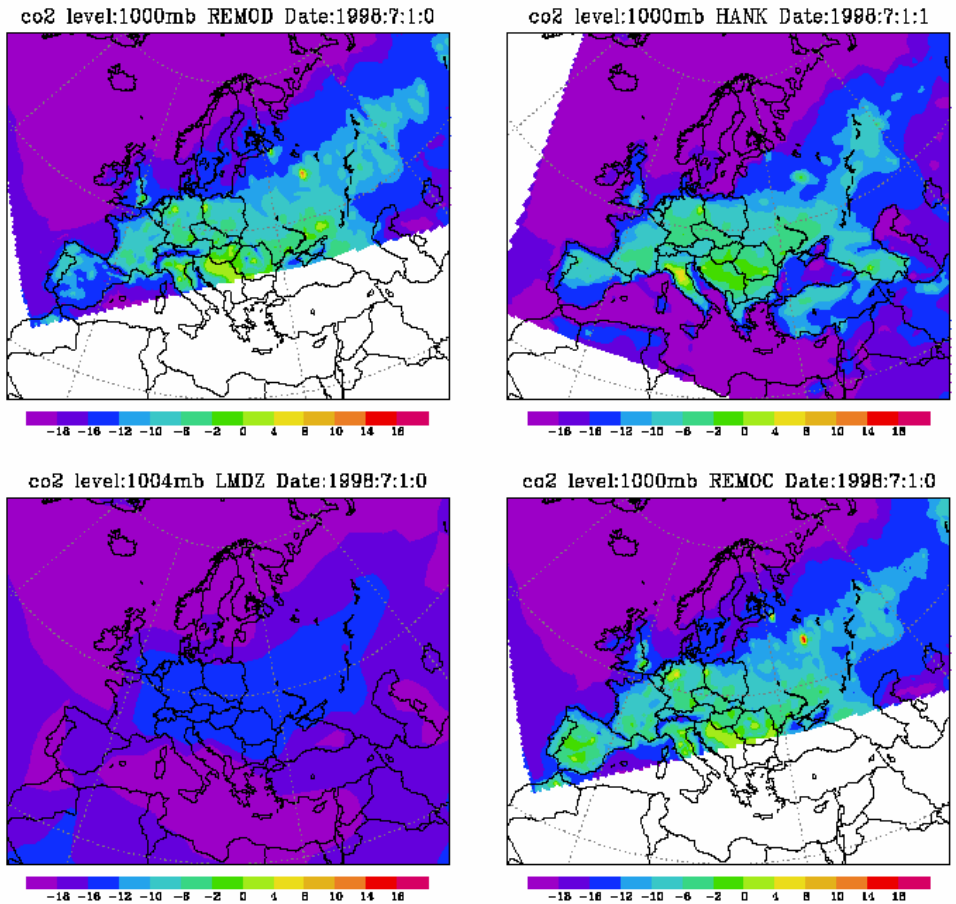

Synthesis inversion of fluxes over European continent

Fluxes a priori
Bio: ORCHIDEE
Anthrop: EDGARxEMEP

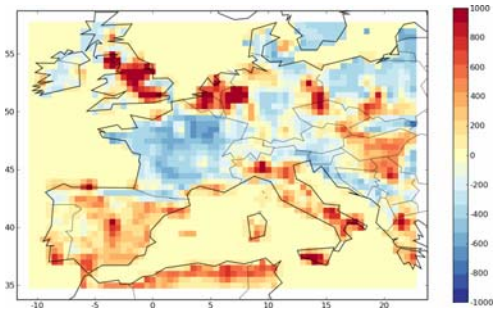

Transport model CHIMERE
(rés. 50 km)

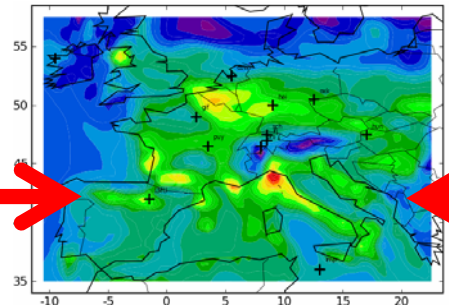

Adjoint of CHIMERE

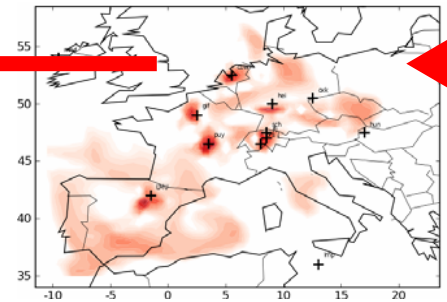

Concentration observations
ICOS network (hourly data)

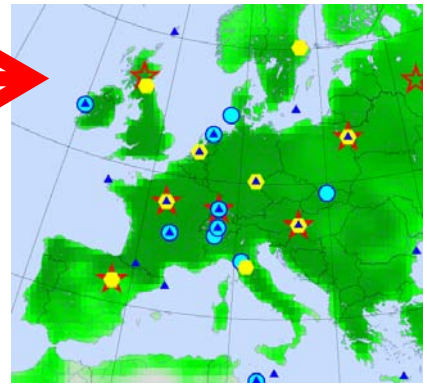

misfit

Corrected fluxes in better agreement with data

Optimized fluxes

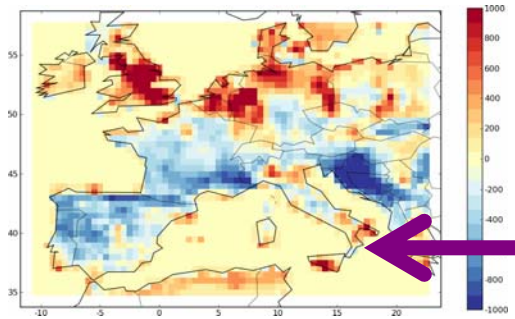

variational data assimilation

Flux increment
rés. 6h / 50 km

Broquet et al. 2011

Inversion of daily land-atmosphere fluxes of CO_2

- Uncertainty reduction from atmospheric data: ~60% on monthly mean fluxes over Europe
- Evaluation of model performances using a) independent concentration data and b) flux measurements

➢ Promising results given the future extension of the ICOS network

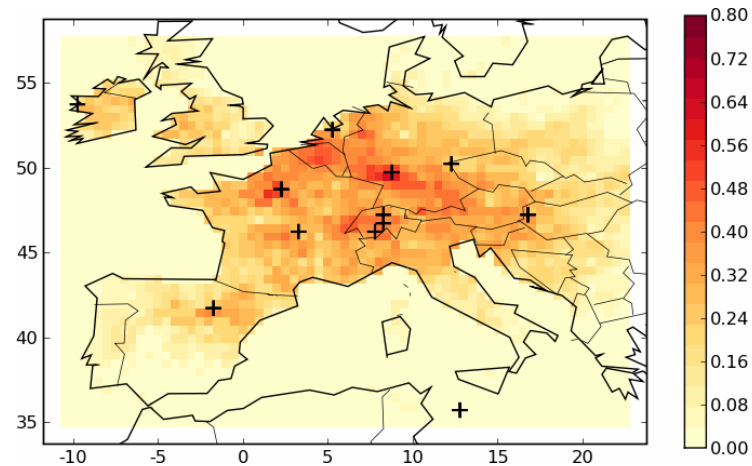

Uncertainty Reduction on monthly fluxes Sumer 2006

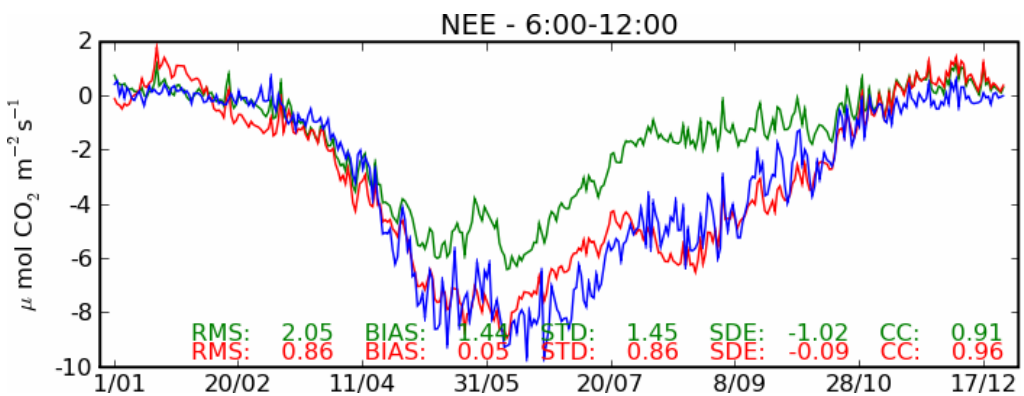

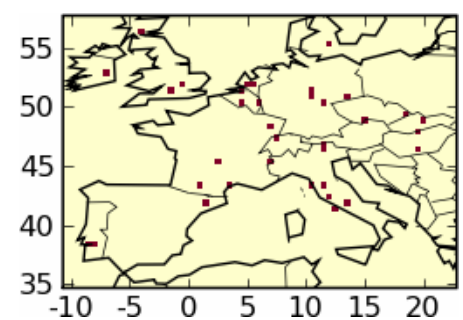

Daily mean fluxes between 6h-12h on model grid compared with local fluxnet sites during summer 2006

Broquet et al. 2011

Local scale inversions (see F Chevallier's)

- Large uncertainties in city scale emissions
- Development of atmospheric network and inverse models to improve cities inventories is a very active research area
- New space missions should allow to characterize cities column CO2 structure(Carbonsat)
- Important economic and political implications

ICOS

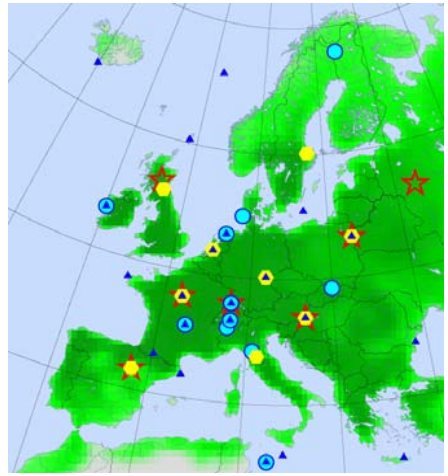

Network around Paris

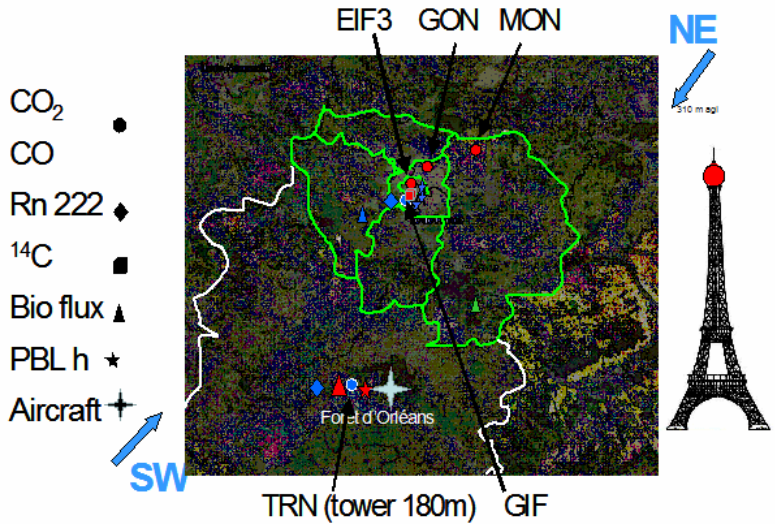

WRF-CHIMERE simulation of the Paris plume at 2 km resolution

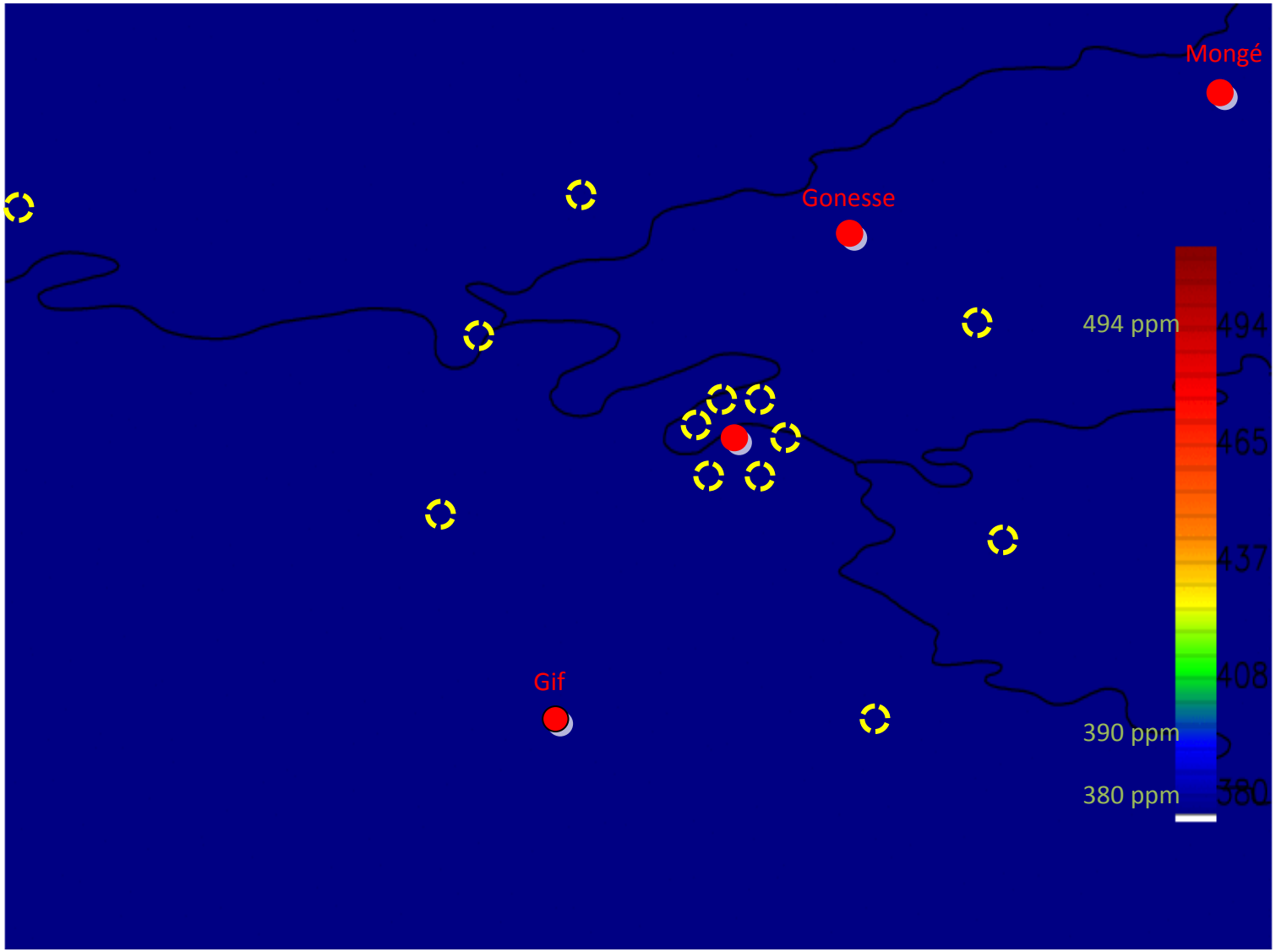

Conclusions

- Inversions are systems, and each part of the system needs to be good for good overall performance
- Global inversions have been applied insofar to quantify the large scale distribution of natural land and ocean fluxes.
- Have shown that the sink balance between NH and Tropics depends critically on atmospheric transport model, with more realistic inversions giving neutral tropical carbon balance.
- Current inversions are limited by data density, but also by transport model errors (at hemispheric, but also at regional scale) ----> Transport models have to be improved over the continents.
- There is only one carbon cycle. There is no reason to assimilate only atmospheric data ----> Development of Carbon cycle data assimilation systems
- Tendency to increase the resolution of inversions down to km for 'verification', which will require information about fossil fuel errors

Continental signals and transport errors

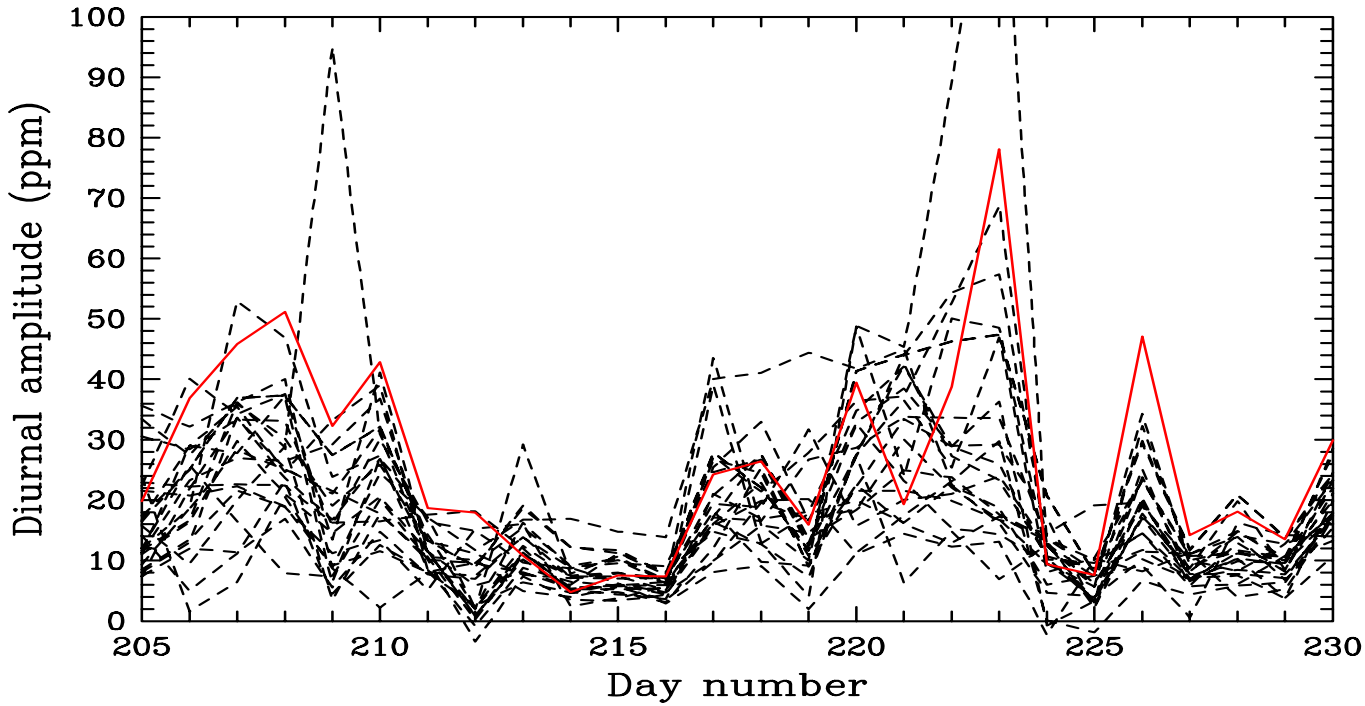

Figure 6. Peak-to-peak diurnal amplitude for 24 July to 18 August 2002 (day 205–230) at BOR for observed CO_2 (red) and modeled CO_2 (black). The amplitude for model IFS for day 223 (139 ppm) is not shown.

Law et al. 2011

Yearly flux estimates
Large regions

Monthly flux estimates
Large regions

Transport model

Coarse global models

Global high resolution models, zoomable or regional models

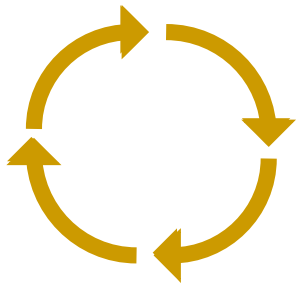

Surface fluxes

Atmospheric concentrations

Yearly observations
MBL & coastal sites

Monthly observations
MBL & coastal sites

Daily to hourly flux estimates
Model resolution (grid 2-50 km)

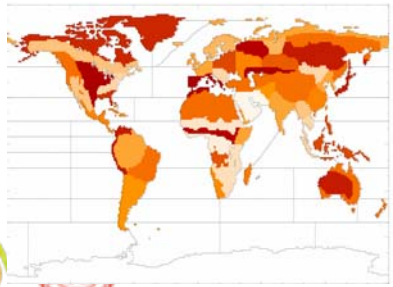

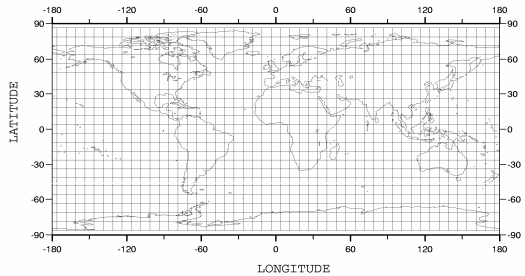

Continuous observations
All sites (included continental)